U.S. DEPARTMENT OF ENERGY

PNNL-22866
DSGREP-RPT-001

Prepared for the U.S. Department of Energy
under Contract DE-AC05-76RL01830

# Prediction of Peak Hydrogen Concentrations for Deep Sludge Retrieval in Tanks AN-101 and AN-106 from Historical Data of Spontaneous Gas Release Events

BE Wells
SK Cooley

Pacific Northwest National Laboratory

JE Meacham

Washington River Protection Solutions, LLC

October 2013

Pacific Northwest
NATIONAL LABORATORY

*Proudly Operated by* Battelle *Since 1965*

**DISCLAIMER**



PACIFIC NORTHWEST NATIONAL LABORATORY
*operated by*
BATTELLE
*for the*
UNITED STATES DEPARTMENT OF ENERGY
*under Contract DE-AC05-76RL01830*

**Printed in the United States of America**

**Available to DOE and DOE contractors from the**
**Office of Scientific and Technical Information,**
**P.O. Box 62, Oak Ridge, TN 37831-0062;**
**ph: (865) 576-8401**
**fax: (865) 576-5728**
**email: reports@adonis.osti.gov**

**Available to the public from the National Technical Information Service**
**5301 Shawnee Rd., Alexandria, VA 22312**
**ph: (800) 553-NTIS (6847)**
**email: orders@ntis.gov <http://www.ntis.gov/about/form.aspx>**
**Online ordering: http://www.ntis.gov**

This document was printed on recycled paper.
(8/2010)

# Prediction of Peak Hydrogen Concentrations for Deep Sludge Retrieval in Tanks AN-101 and AN-106 from Historical Data of Spontaneous Gas Release Events

BE Wells
SK Cooley

Pacific Northwest National Laboratory

JE Meacham

Washington River Protection Solutions, LLC

October 2013

Prepared for
the U.S. Department of Energy
under Contract DE-AC05-76RL01830

Pacific Northwest National Laboratory
Richland, Washington 99352

# Summary

Radioactive and chemical wastes from nuclear fuel processing are stored in large underground storage tanks at the Hanford Site. The Tank Operations Contractor is continuing a program of moving solid wastes from single-shell tanks (SSTs) to double-shell tanks (DSTs) and preparing for waste feed delivery (WFD). A new mechanism for a large spontaneous gas release event (GRE) in deep sludge sediments has been postulated. This potential new GRE hazard, deep sludge gas release events (DSGREs), can be created by the retrieval of sludge waste into a single DST that results in a sediment depth greater than previous operating experience has demonstrated is safe. The Tank Operations Contractor program of moving solid wastes from SSTs to DSTs and preparing for WFD is being negatively impacted by this sediment depth limit.

One approach to evaluate the hazard is to estimate the effect of this new waste configuration relative to the spontaneous GRE events that have been observed in the Hanford tank farms, the largest of which are attributed to buoyant displacement gas release events (BDGREs). An empirical model based on tank farm spontaneous GRE data and waste properties to predict the flammable gas (specifically hydrogen) concentration in a tank's headspace is available. This flammability model is applied in this report to the anticipated conditions resulting from C Tank Farm sludge retrieval into Tanks AN-101 and AN-106. Based on historical Hanford waste spontaneous gas release volumes, the allowed depth of sludge in Tanks AN-101 and AN-106 are determined that will limit headspace hydrogen concentrations to a given fraction of the lower flammability limit (LFL).

For the projected retrievals of C Tank Farm waste into AN Tank Farm, there are no actual waste data, and the waste characteristics have been estimated. Tank waste data are available from a variety of sources, but has a degree of uncertainty associated with it. The magnitude of this uncertainty is affected by a number of factors, such as waste heterogeneity, analysis methodology and equipment, and incomplete or missing data. To account for the uncertainty in the data, the parameter values used in this study have been assigned distributions that reflect the uncertainty in the estimation of the various tank waste properties. A Monte Carlo methodology was employed to calculate simulated distributions of sediment depth values (as it relates to the flammability model).

The flammability model is based on the large BDGREs that occur in a limited number of the Hanford waste tanks. The projected waste characteristics for retrievals of C Tank Farm waste into AN Tank Farm were evaluated with respect to the flammability model bases, and it was concluded that no adjustments were necessary to account for waste property differences.

From the Monte Carlo simulations performed with the flammability model, the allowable sediment depth to prevent spontaneous GREs from exceeding 100% of the LFL was calculated to be 280 in. in Tank AN-101 and 226 in. in Tank AN-106. The bases for these predictions are the gas release behaviors of the BDGRE tanks. Therefore, these model results should only be used in combination with other planned studies of DSGRE behavior to address the range of potential releases. If the gas releases from DSGREs are indicated by the other planned studies to be smaller than would be expected for BDGREs, the flammability model bounds the potential gas releases from the deep sludge in Tanks AN-101 and AN-106.

# Acknowledgments

The authors thank JA Fort for his independent technical review, SA Suffield for her calculation reviews, and KR Neiderhiser for the document production.

# Acronyms and Abbreviations

| | |
|---|---|
| BDGRE | buoyant displacement gas release event |
| DSA | Documented Safety Analysis |
| DSGRE | deep sludge gas release event |
| DST | double-shell tank |
| GRE | gas release event |
| LFL | lower flammability limit |
| PNNL | Pacific Northwest National Laboratory |
| SST | single-shell tank |
| UDS | undissolved solids |
| WFD | waste feed delivery |
| WTP | Hanford Tank Waste Treatment and Immobilization Plant |

# Contents

Summary ..... iii
Acknowledgments ..... v
Acronyms and Abbreviations ..... vii
1.0 Introduction ..... 1.1
1.1 Approach ..... 1.3
1.2 Quality Requirements ..... 1.3
2.0 Spontaneous Gas Release Volume Model ..... 2.1
2.1 Model ..... 2.1
2.2 Model Applicability ..... 2.4
3.0 Waste Characteristics and Model Effects ..... 3.1
3.1 Monte Carlo Approach ..... 3.2
3.2 Layer Densities ..... 3.3
3.3 Layer Depth and Temperature ..... 3.8
3.4 Gas Generation and Composition ..... 3.10
3.5 Sediment Rheology ..... 3.13
3.5.1 Waste Rheology Data ..... 3.14
3.5.2 Effect of Waste Rheology on Flammability Model ..... 3.18
4.0 Results ..... 4.1
4.1 Effect of Simulation Approach ..... 4.1
4.2 Parameter Sensitivity ..... 4.2
4.2.1 Effect of Hydrogen Concentration in the Retained Gas ..... 4.2
4.2.2 Effect of Peak Hydrogen Concentration in Headspace Limit ..... 4.4
4.3 Discussion ..... 4.5
5.0 Conclusions ..... 5.1
6.0 References ..... 6.1

# Figures

2.1. Quadratic and Linear Models for 95th Percentile Peak [$H_2$], Stewart et al. (2005) ..... 2.3
3.1. Tank AN-101 Liquid Density Distribution (kg/m$^3$) ..... 3.5
3.2. Tank AN-106 Liquid Density Distribution (kg/m$^3$) ..... 3.6
3.3. Calculated Sediment Density ..... 3.7
3.4. Calculated Neutral Buoyancy Gas Fraction ..... 3.8
3.5. Tank AN-101 Hydrogen Generation Rate Distribution (mols/m$^3$/day). ..... 3.11
3.6. Tank AN-106 Hydrogen Generation Rate Distribution (mols/m$^3$/day). ..... 3.12
3.7. Hydrogen Concentration in Retained Gas Distribution (volume fraction). ..... 3.13
3.8. Data Summary of C Tank Farm Shear Vane Shear Strength ..... 3.15
3.9. Stress-Strain for Bentonite Clay (Stewart et al. 1996) ..... 3.16
3.10. Stress-Strain for Chemical Simulant S2 ..... 3.17
3.11. Chemical Simulants Strain at Failure ..... 3.17
3.12. Comparison of Projected Sludge and BDGRE Tanks $m_\tau$ ..... 3.21
3.13. Comparison of Projected Sludge and BDGRE Tanks $m_\tau$ and $\tau\varepsilon$ ..... 3.22
4.1. H2 Case 1 (LFL Case 1, see Section 4.2.2) ..... 4.3
4.2. H2 Case 2 ..... 4.3
4.3. H2 Case 3 ..... 4.4
4.4. LFL Case 2 ..... 4.5

# Tables

3.1. Projected Contribution Fractions to Sediment Depth ..... 3.1
3.2. Liquid Density Distributions (kg/m$^3$) ..... 3.6
3.3. Hydrogen Generation Rate Distributions (mols/m$^3$/day) ..... 3.12

# 1.0 Introduction

Radioactive and chemical wastes from nuclear fuel processing are stored in large underground storage tanks at the Hanford Site. There are 149 older single-shell tanks (SSTs) built in the 1940s through 1960s and 28 newer double-shell tanks (DSTs) built in the 1970s and 1980s. The SSTs contain little drainable liquid waste and the Tank Operations Contractor is continuing a program of moving solid wastes from SSTs to DSTs and preparing for waste feed delivery (WFD). The Hanford DST system also provides the staging location for WFD to the Hanford Tank Waste Treatment and Immobilization Plant (WTP).

Some DSTs store only liquid waste, while others contain both liquid and a layer of settled solids or sediment. Solid wastes can be classified as saltcake or sludge. Saltcake is mostly soluble sodium nitrate and nitrite salts with some interstitial liquid consisting of concentrated salt solutions. Sludge is mostly low solubility aluminum and iron compounds with relatively dilute interstitial liquid (Meacham et al. 2012).

As summarized in Meacham and Kirch (2013), the Documented Safety Analysis (DSA) (Kripps 2011) considers two mechanisms by which waste-generated flammable gases can reach high concentrations in tank farm facilities. First, flammable gases generated by the waste are continuously released into tank vapor spaces. In the absence of adequate ventilation, the steady-state concentration of these gases can potentially exceed the lower flammability limit (LFL). Second, a fraction of the gas generated by the waste can be retained within the sediment. This retained gas can be released in a spontaneous or induced gas release event (GRE) thereby increasing the flammable gas concentration in a tank headspace to above the LFL. The DSA states that

> "Large, spontaneous GREs are caused by a phenomena called "buoyant displacement" and can occur in tanks with a deep layer of supernatant when a portion or "gob" of the settled solids accumulates sufficient gas to become buoyant with respect to the liquid above it, breaks away, and rises through the liquid. The stored gas bubbles expand as the gob rises, disrupting the surrounding waste so a portion of the gas can escape into the tank headspace. Large spontaneous GREs have resulted in flammable concentrations only three times. These occurred in DST 241-SY-101 prior to remediation. The mechanisms for spontaneous gas releases from waste without supernatant are less understood but probably are the result of "percolation" of individual bubble systems. The potential volume of this kind of release is orders of magnitude smaller than that of a buoyant displacement GRE."

The DSA also states in reference to buoyant displacement gas release events (BDGREs),

> "Relatively weak, wet waste is capable of retaining a significant volume of gas and can release large fractions of it suddenly."

Meacham and Kirch (2013) postulated a new mechanism for a large spontaneous GRE in deep sludge sediments that is not currently described in the DSA. This new mechanism is referred to as a deep sludge gas release event (DSGRE). Meacham and Kirch (2013) referenced studies that suggest there is a limit to the depth of the connected pathways that allow gas to escape and limit gas retention in sludge waste that

exhibits the properties of "stiff waste." Thus, there is a limit to the depth of sludge that can release its gas without causing a spontaneous GRE.

The referenced studies of van Kessel and van Kesteren (2002) were performed with dredging sludge from contaminated lake bottoms and found these pathways or channels could be stable to a depth of 8 to 10 meters (320 to 390 in.). If the depth of sludge exceeds the depth of the connected pathways, gas can be retained in the lower region of sludge (below the sludge with connected pathways) until the gas fraction reaches the point that the lower sludge matrix becomes unstable. Meacham and Kirch (2013) postulated that the density difference caused by the void difference results in upwelling of the lower layer and downward motion of the upper layer and that a spontaneous gas release could occur because of this motion. Whether this phenomena will occur in Hanford sludge sediment, and what the size and rate of gas release from any such DSGRE may be are not known, and this mechanism is different from the "buoyant displacement" phenomena described in the DSA.

The DSGRE issue was identified in WRPS-PER-2012-2007 (2012), evaluated by the Plant Review Committee as documented in Occurrence Report EM-RP--WRPS-TANKFARM-2012-0014, and declared to be a Potential Inadequacy in the Safety Analysis. A Red Arrow was established in the Base Operations Central Shift Office logbook as a compensatory measure to prevent GREs from DSGREs. The Red Arrow states, "Planned waste transfers into DSTs that could result in a settled sludge depth greater than 170 inches (as measured by sludge weight assembly) are prohibited unless the DST remains Waste Group C (described below) using the approved methodology in RPP-10006 [Yarbrough, 2013]."

The DSA controls that prevent potential GRE flammable gas hazards from large spontaneous BDGREs may not preclude a large spontaneous GRE from DSGREs. The controls derived to prevent potential GRE flammable gas hazards are based on evaluations and observations of gas retention and release behavior in tank farm waste contained in documents prepared to support resolution of the flammable gas safety issue and in documents developed specifically to support GRE flammable gas hazard control decisions.

The methodology and calculations performed to classify a Hanford waste tank as a BDGRE tank are described in Yarbrough (2013). Yarbrough (2013) provides three criteria for preventing BDGRE flammable gas hazards: 1) retained gas volume, 2) energy ratio, and 3) buoyancy ratio. The retained gas volume criterion is used to determine the tanks where there is no potential GRE flammable gas hazard no matter what the gas release mechanism is (i.e., Waste Group C) as there is not enough retained gas present in these tanks to reach the LFL even if all of it were to be instantly released. The energy ratio (Stewart et al. 1996; Meyer et al. 1997) and buoyancy ratio (Meyer and Stewart 2001; Stewart et al. 2005) criteria are then used to determine the non-Waste Group C tanks with a potential spontaneous BDGRE flammable gas hazard in addition to a potential induced GRE flammable gas hazard (i.e., Waste Group A). Control of the GRE hazard by controlling the energy ratio assumes that a shallow supernatant layer will lead to a low energy ratio and, therefore, control the spontaneous GRE hazard.

As discussed in Meacham and Kirch (2013), Hanford Tank Farm operating experience demonstrates that significant gas retention and spontaneous GREs have not been observed in deep settled sludge. Therefore, the limiting depth of sludge for the postulated DSGRE scenario to occur is hypothesized to be greater than the current sludge depth in the DSTs and SSTs. Preliminary theoretical analyses for DST waste sludges (Meacham 2010) estimated that the depth of sludge that maintains its connected pathways

ranges from 4.4 to 9.8 meters (173 to 386 in.) via the Winterwerp and van Kesteren (2004) model for dredging sludge and assumed Hanford waste values.

The controls derived to prevent potential BDGRE flammable gas hazards (see Yarbrough 2013), specifically the energy ratio, may not preclude a large spontaneous GRE from DSGREs. The postulated DSGRE mechanism for spontaneous GRE in "stiff wastes" is thought to be independent of the depth of supernatant liquid; therefore, it is not prevented by controlling to a low energy ratio.

## 1.1 Approach

The postulated DSGRE phenomena is currently an issue due to the retrieval of sludge waste into a single DST that results in a sediment depth greater than operating experience has demonstrated is safe. The Tank Operations Contractor program of moving solid wastes from SSTs to DSTs and preparing for WFD is being negatively impacted by this sediment depth limit. One approach to evaluate the hazard is to estimate the effect of this new waste configuration relative to the spontaneous GRE events that have been observed in the Hanford tank farms, the largest of which are attributed to BDGREs (Hedengren et al. 2000).

Stewart et al. (2005) provides an empirical model based on tank farm spontaneous GRE data and waste properties to predict the flammable gas (specifically hydrogen) concentration in a tank's headspace. In this report, the Stewart et al. (2005) model is applied to the anticipated conditions resulting from C Tank Farm sludge retrieval into Tanks AN-101 and AN-106 to determine the limit of sediment depth that can be present in those tanks such that estimated spontaneous GREs result in a hydrogen concentration in the headspace below a given limit. The Stewart et al. (2005) model is based on the large BDGREs that occur in a limited number of the Hanford waste tanks (Hedengren et al. 2000). Therefore, the results can be used to support a basis for the safe storage of increased sediment depths in Tanks AN-101 and AN-106 relative to the largest GREs from tank farms operational data. The specific objective of this report is:

> Based on historical Hanford waste spontaneous gas release volumes, determine the allowed depth of sludge in Tanks AN-101 and AN-106 that will limit headspace hydrogen concentrations to a given fraction of the LFL.

The model results should only be used in combination with other planned studies of DSGRE behavior to address the range of potential releases.

## 1.2 Quality Requirements

This work is required to comply with all NQA-1 requirements and quality clauses as specified in the Statement of Work.

The Pacific Northwest National Laboratory (PNNL) Quality Assurance Program is based upon the requirements as defined in the U.S. Department of Energy (DOE) Order 414.1D, "Quality Assurance" and Title 10 *Code of Federal Regulations* (CFR) Part 830, "Nuclear Safety Management," Subpart A – "Quality Assurance Requirements" (a.k.a. the Quality Rule). PNNL has chosen to implement the following consensus standards in a graded approach:

- ASME NQA-1-2000, Quality Assurance Requirements for Nuclear Facility Applications, Part I, Requirements for Quality Assurance Programs for Nuclear Facilities.
- ASME NQA-1-2000, Part II, Subpart 2.7, Quality Assurance Requirements for Computer Software for Nuclear Facility Applications.
- ASME NQA-1-2000, Part IV, Subpart 4.2, Guidance on Graded Application of Quality Assurance (QA) for Nuclear-Related Research and Development.

The procedures necessary to implement the requirements are deployed through PNNL's "How Do I…? (HDI) system for delivering requirements to PNNL staff.

The work contained herein was performed in accordance with 64405-QA-001, *Support to Evaluation of Gas Release Mechanisms in Deep Sludge Project Quality Assurance Plan*. The Deep Sludge Gas Release Event Project uses the Washington River Protection Solutions (WRPS) Waste Form Testing Program (WWFTP) QA program (QA-WWFTP-001) at the Applied Research level as the basis for performing work. The WWFTP QA program implements an NQA-1-2000 quality assurance program, graded on the approach presented in NQA-1-2000, Part IV, Subpart 4.2. This QA program and implementing procedures meet the quality requirements of NQA-1-2004, NQA-1a-2005, and NQA-1b-2007 as provided in the Statement of Work authorizing PNNL to conduct these studies.[1]

The analyses were performed using Microsoft Excel and R. Calculations were performed with functions integral to that software. The preparation, content, review, and approval of Calculation Packages including both hand calculations and computer-assisted calculations (CCPs) were performed in accordance with QA-NSLW-0304.

[1] This program has been independently evaluated by Acquisition Verification Services (AVS) of Mission Support Alliance (MSA) to specified requirements of NQA-1:2004 (including NQA-1a-2005 and NQA-1b-2007 Addenda) and is operating under WRPS-approved Supplier Quality Assurance Program Implementation Plan (SQAPIP) QA-WWFTP-002.

# 2.0 Spontaneous Gas Release Volume Model

Stewart et al. (2005) present a method for predicting the potential flammability resulting from a specific kind of spontaneous GRE, specifically BDGREs, that occur in a few of the Hanford radioactive waste storage tanks. As described in Section 1, BDGRE models have been incorporated into the DSA as described by Yarbrough (2013). A summary of the Stewart et al. (2005) is provided in Section 2.1 and the model applicability relative to the properties of the waste being evaluated is discussed in Section 2.2.

## 2.1 Model

The Stewart et al. (2005) methodology formally correlates the buoyancy ratio (Meyer and Stewart 2001; Yarbrough 2013) and the peak headspace hydrogen concentration resulting from BDGREs (Hedengren et al. 2000; Wells et al. 2002). This flammability model can be used to relate the buoyancy ratio to a limiting headspace hydrogen concentration.

The buoyancy ratio model was developed based on observations of Hanford tank farm data that 1) the gas volume fraction generally increased downward from essentially zero at the top of the sediment and sometimes followed a parabolic profile with a maximum below the sediment midplane, 2) the sediment yield stress increased linearly downward from zero at the top of the sediment, and 3) the gas fraction profiles in the sediment were often very dissimilar at different locations in the tank. The causes of all three of these observations are interrelated. Also, because gas is generated continuously and uniformly throughout the waste but only a few tanks retain enough gas to have BDGREs, there must be a slow, almost imperceptible bubble migration up through the sediment that releases the generated gas in most tanks before it becomes buoyant.

By combining expressions for the bubble migration velocity and the variation in gas volume with elevation in the sediment as described by one-dimensional conservation equations for the bubble mass and number, an equation describing the gas fraction profile in the sediment can be defined. Integrating the gas fraction profile from the top of the sediment downward and dividing by the neutral buoyancy gas fraction (the gas fraction required to make the sediment neutrally buoyant with respect to the overlaying supernatant liquid layer) yields the buoyancy ratio

$$BR = \frac{C}{\rho_S - \rho_L}\left(\frac{GT_S}{p_{gas}}\right)^{1/3} H_S^2 \qquad (2.1)$$

where
- $\rho_S$ = sediment density (kg/m$^3$)
- $\rho_L$ = liquid density (kg/m$^3$)
- $G$ = gas generation rate (mols/m$^3$/day), $G=H/[H_2]_{gas}$
- $H$ = hydrogen gas generation rate (mols/m$^3$/day)
- $[H_2]_{gas}$ = hydrogen fraction in retained gas
- $T_S$ = average sediment temperature (K)
- $p_{gas}$ = average gas pressure in the sediment (Pa)
- $H_S$ = sediment layer depth (m)

and the leading coefficient is the calibration factor, C, which contains all of the constants and unknowns is

$$C = \left[ \frac{3}{16} \frac{N^{2/3} R^{1/3} m_\tau}{SKg} \right]$$

where
- $N$ = bubble nucleation rate per unit volume
- $R$ = gas constant (8314 J/mole-K)
- $m_\tau$ = slope of the yield stress as a function of sediment depth (Pa/m)
- $S$ = proportionality constant for true Stokes flow, $S = \frac{2}{9}\left(\frac{3}{4\pi}\right)^{\frac{2}{3}}$
- $K$ = unknown proportionality constant between the effective viscosity and yield stress in shear
- $g$ = gravitational acceleration ($m/s^2$).

The calibration factor, C, for use in the flammability model is specified in Stewart et al. (2005) to be 21.8293 ($kg/m^4$) (day-atm/mol-K)$^{1/3}$, or 1,018 ($kg/m^4$) (day-Pa/mol-K)$^{1/3}$ (with the average gas pressure in the sediment expressed in Pa), when the minimum buoyancy ratio for the BDGRE tanks was set to unity.[1] The average gas pressure in the sediment is estimated using the expression in Yarbrough (2013) as

$$p_{gas} = P_A + \rho_L g\left( H_L + \frac{H_S}{2} \right) \tag{2.2}$$

where
- $P_A$ = atmospheric pressure, 101,325 (Pa)
- $H_L$ = liquid layer depth (m).

The Stewart et al. (2005) flammability model thus relates tank behavior (spontaneous GREs) to tank conditions (as described by the parameters of the buoyancy ratio, Equation (2.1)), for a variety of data and observations. Stewart et al. (2005) studied the available data on the six historic BDGRE tanks in great detail to provide the best possible description of their waste state and the distribution of BDGREs that the tanks produced.

The variability in the BDGRE sizes and the uncertainty in the tank data were included in deriving the model through a Monte Carlo simulation. Uncertainty distributions were developed for each of the important variables used in calculating the buoyancy ratio. The BDGRE history, in terms of gas release volume, for each tank was fit with a distribution from which the 95$^{th}$ percentile value was extracted to represent the maximum expected gas release. A function of the buoyancy ratio involving the headspace volume and hydrogen fraction of the retained gas was fit to these 95$^{th}$ percentile BDGREs using a simple quadratic model. The buoyancy ratio criterion was then derived from the upper bound of the 95% confidence limit for the model fit.

The headspace volume and hydrogen fraction of the retained gas for the respective tanks were required to normalize the BDGRE gas release volumes to hydrogen concentration. The flammability

[1] The six Hanford waste tanks on which the flammability model is based are AN-103, AN-104, AN-105, AW-101, SY-103, and SY-101.

model thus relates the expected peak headspace hydrogen concentration from a spontaneous GRE in a tank to the calculated buoyancy ratio, tank headspace volume, and fraction of hydrogen in the retained gas.

The limiting buoyancy ratio criterion is derived from the upper bound of the 95% confidence interval of the best quadratic model fit to the 95$^{th}$ percentile peak hydrogen concentration estimates shown in Figure 2.1. The equation describing the upper bound of the 95% confidence interval of the quadratic model is given by

$$0.01895\mathrm{f}(\mathrm{BR})^2 + 18.01\mathrm{f}(\mathrm{BR}) + 14432 = [\mathrm{H_2}]_{\mathrm{peak}} \tag{2.3}$$

where $f(BR) = 10^6(BR-1)[H_2]_{gas}/V_{HS}$; $[H_2]_{peak}$ is the set limit for the maximum headspace hydrogen concentration and $V_{HS}$ is the headspace volume. Solving Equation (2.3) for the buoyancy ratio gives

$$\mathrm{BR} = 1 + \frac{\mathrm{V_{HS}}}{3.79\left(10^4\right)\left[\mathrm{H_2}\right]_{\mathrm{gas}}}\left\{-18.01 + \sqrt{324.18 - 0.0758\left(14432 - \left[\mathrm{H_2}\right]_{\mathrm{peak}}\right)}\right\} \tag{2.4}$$

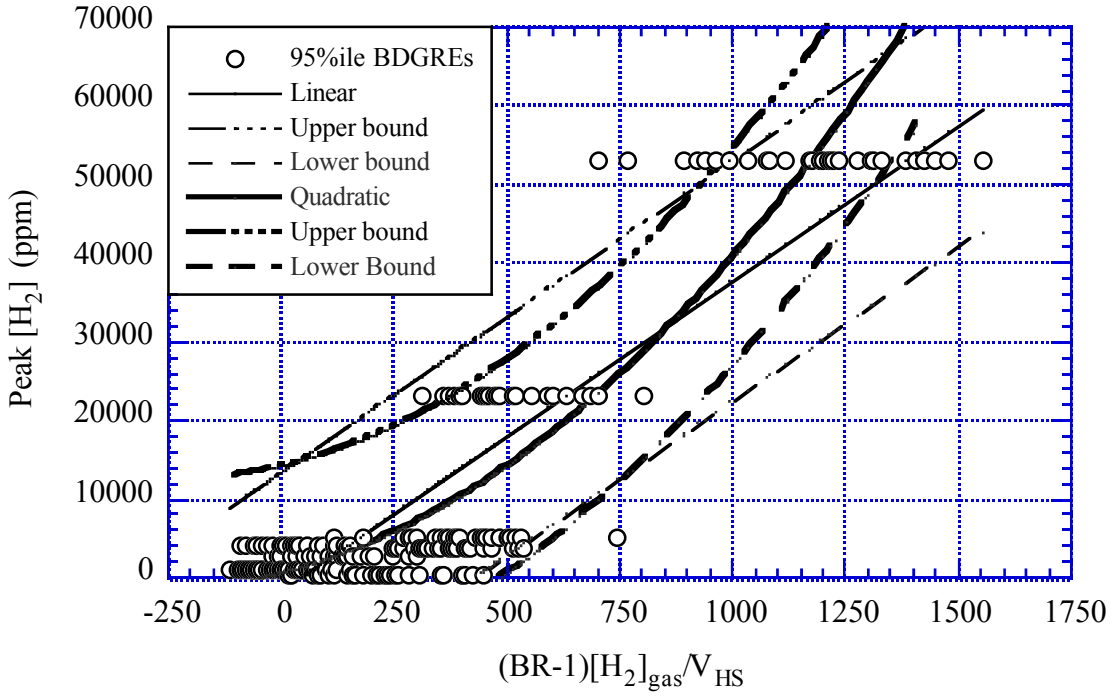


**Figure 2.1**. Quadratic and Linear Models for 95$^{th}$ Percentile Peak $[H_2]$, Stewart et al. (2005). Equation (2.3) describes the quadratic upper bound.

Equation (2.4) defines the limiting value of the buoyancy ratio for a given maximum hydrogen concentration, $[H_2]_{peak}$. The limit can be set to the LFL for hydrogen, 40,000 ppm, a value accounting for the presence of other fuel gases calculated via LeChatelier's law, or some lower concentration like 60% LFL. Besides the limiting hydrogen concentration, the limiting buoyancy ratio depends on the retained gas hydrogen volume fraction as well as the tank headspace.

The minimum value for the hydrogen concentration which gives a buoyancy ratio of 1.0 is approximately 14,400 ppm using waste parameters for Tank AN-103 from Stewart et al. (2005) in Equation (2.3) (see Figure 2.1). In contrast, the largest measured peak hydrogen concentration reported in Hedengren et al. (2000) for Tank AN-103 is 1,600 ppm, so the 14,400 ppm is an over-prediction of the model at lower buoyancy ratios (i.e., lower BR-1), which is clearly evident in Figure 2.1. For higher buoyancy ratio tanks, the model represents the lower BR results for the 95$^{th}$ percentile peak hydrogen concentration estimates from the tank farm data (Figure 2.1). These conservative (higher than measured or higher than typical hydrogen concentration resulting from spontaneous GREs) results from the flammability model of Equation (2.3) are the result of the model being based on the upper bound of the 95% confidence interval of the best quadratic model fit to the 95$^{th}$ percentile peak hydrogen concentration estimates of the six BDGRE tanks.

The enabling assumption for the flammability model is the acknowledgment that the BDGREs now occurring in five tanks are not hazardous. This realization allows specification of a limiting buoyancy ratio that is greater than unity, allowing for the occurrence of inconsequential BDGREs but preventing the hazardous events.

## 2.2 Model Applicability

The major assumptions used to derive the buoyancy ratio-based models were based on data from the six BDGRE tanks. The range of data representing the six BDGRE tanks is quite narrow. Their waste physical properties are very similar (Hedengren et al. 2000), and the sediment yield stress is relatively low typically in comparison to sludge wastes (Stewart et al. 2005). The difference between sediment and liquid densities is small and the waste composition represents concentrated saltcake. A detailed study of the range of applicability of the flammability model and of the previous buoyancy ratio criterion for preventing BDGREs was performed by Stewart et al. (2005). A basis for the application of the models is described by Stewart et al. (2005) for a range of sediment conditions, and those sediment conditions (i.e., difference from the model bases) expected to be of potential significance to the current issue of waste retrieval into DSTs to form deep sludge layers are:

- deep sediment (Section 3.3)
- uniform sediment yield stress in shear with depth; the yield stress in shear or shear strength increases approximately linearly with depth in the BDGRE tanks, and this is a key assumption in the buoyancy ratio model (Section 3.5)
- strong sediment; the yield stress in shear or shear strength is greater than measured for the BDGRE tanks (Section 3.5)
- brittle sediment; the strain at failure is less than that postulated for the BDGRE tanks (Section 3.5).

As described in Stewart et al. (2005), these waste characteristic differences may require adjustment of the flammability model. In Section 3, the expected retrieved waste characteristics are defined, and a determination is made, relative to these properties, of their effect on the model.

# 3.0 Waste Characteristics and Model Effects

The parameters required for the Stewart et al. (2005) spontaneous GRE flammability model are listed in Section 2. Tank waste data are available from a variety of sources, but, regardless of the source, tank waste information has a degree of uncertainty associated with it. The magnitude of the uncertainty is affected by a number of factors, such as waste heterogeneity, analysis methodology and equipment, and incomplete or missing data. For the projected retrievals of C Tank Farm waste into AN Tank Farm, there are no actual data, and therefore the waste characteristics must be estimated.

To account for the uncertainty in the data, the values used in this study have been assigned distributions that reflect the uncertainty in the estimation of the various tank waste properties and a Monte Carlo methodology is employed to calculate results. Section 3.1 describes the Monte Carlo approach. The flammability model parameter values and developed distributions are presented in the subsequent sections. Where pertinent, as defined in Section 2.2, the effect of the waste characteristics relative to the flammability model bases are investigated.

The expected waste properties at the end of the projected retrievals in Tanks AN-101 and AN-106 are developed from the available characterizations of the C Tank Farm and AN Tank Farm wastes (with consideration of other Hanford sludge waste data) as they are projected to be combined. Based on past characterizations (Hu 2006), transfer records,[1] and projected retrieval volumes (Uytioco 2011; Barton et al. 2013), the fractions of each C Tank Farm and AN Tank Farm tank that comprise the resultant AN Tank Farm sediments can be estimated as listed in Table 3.1. C Tank Farm tanks C-104, C-111, C-112, C-101, and C-102 have been, are being, or are planned to be retrieved into Tank AN-101, while Tanks C-108, C-107, C-110, C-109, and C-105 are associated with Tank AN-106. The retrievals are not sequential in that waste from one C Tank Farm tank may be retrieved into an AN Tank Farm tank, followed by waste from a different C Tank Farm tank or tanks, followed by waste from the first C Tank Farm tank, and so on. Thus, the resultant AN Tank Farm sediments are likely layered, but the exact waste compositions in the original C Tank Farm tank may not be uniquely preserved.

**Table 3.1**. Projected Contribution Fractions to Sediment Depth

| Tank | Sediment Fraction by Volume |
|---|---|
| **AN-101** | 0.060 |
| C-104 | 0.314 |
| C-111 | 0.040 |
| C-112 | 0.131 |
| C-101 | 0.081 |
| C-102 | 0.374 |
| **AN-106** | 0.153 |
| C-108 | 0.053 |
| C-107 | 0.301 |
| C-110 | 0.218 |
| C-109 | 0.062 |
| C-105 | 0.213 |

[1] Tank Waste Information System (TWINS) database (http://twins.pnl.gov/twins3/twins.htm).

## 3.1 Monte Carlo Approach

A Monte Carlo simulation was conducted to generate simulated distributions of sediment depth values (as it relates to the flammability model) for conditions representative of waste in Tanks AN-101 and AN-106. For each combination of input parameters, the sediment height that will limit headspace hydrogen concentrations to a given fraction of the LFL is determined. The buoyancy ratio is calculated from Equation (2.4), the flammability model, which provides a buoyancy ratio such that the headspace hydrogen concentration is limited to the specified fraction of the LFL. The buoyancy ratio is also calculated from Equation (2.1), and the sediment height is adjusted such that the buoyancy ratio calculated from both Equation (2.4) and Equation (2.1) is equivalent. This sediment height is, therefore, the limiting depth for a specified LFL limit based on the flammability model.

The methodology includes calculations that involve combinations of the input variables liquid density ($\rho_L$, Section 3.2); hydrogen gas generation rate (H, Section 3.4); and hydrogen fraction in retained gas ($[H_2]_{gas}$, Section 3.4), that describe potential tank conditions for Tanks AN-101 and AN-106. The particular combinations of $\rho_L$, H, and $[H_2]_{gas}$ values used to generate the simulated sediment depths were randomly selected from larger domains of possible combinations of $\rho_L$, H, and $[H_2]_{gas}$ values that represent ranges of potential conditions in Tanks AN-101 and AN-106, respectively. That is, the domain of possible combinations of $\rho_L$, H, and $[H_2]_{gas}$ for Tank AN-101 was the set of all possible 3-tuples that results from crossing representative distributions of $\rho_L$, H, and $[H_2]_{gas}$ values that describe conditions in Tank AN-101. Similarly, the domain of possible combinations of $\rho_L$, H, and $[H_2]_{gas}$ for Tank AN-106 was the set of all possible 3-tuples that results from crossing representative distributions of $\rho_L$, H, and $[H_2]_{gas}$ values that describe conditions in Tank AN-106.

The representative distributions of $\rho_L$, H, and $[H_2]_{gas}$ contained values for each of these random variables based on specified targets for median value, range of values, and general shape of the distribution. The characteristics describing the target distributions were based on existing tank farm data relative to these random variables (see Section 3.2 and Section 3.4).

Each of the representative distributions contains 5,000 values. Thus, the domain of possible 3-tuple combinations of $\rho_L$, H, and $[H_2]_{gas}$ available for determining sediment depth for each tank contained $5{,}000^3$ or $1.25 \times 10^{11}$ combinations. Rather than performing calculations to determine sediment depths for Tanks AN-101 and AN-106 using all $1.25 \times 10^{11}$ available combinations of corresponding input variables for each tank, a random sample of 5,000 combinations of $\rho_L$, H, and $[H_2]_{gas}$ was generated and used to determine 5,000 simulated sediment depth values for Tank AN-101, and a separate random sample of 5,000 combinations of $\rho_L$, H, and $[H_2]_{gas}$ was generated and used to determine 5,000 simulated sediment depth values for Tank AN-106. In generating these random samples, the variables $\rho_L$, H, and $[H_2]_{gas}$ were assumed to be uncorrelated.

The random sample of 5,000 combinations of $\rho_L$, H, and $[H_2]_{gas}$ used for determining simulated sediment depth for Tank AN-101 was generated as follows (and depicted schematically):

- The 5,000 realizations from the representative distributions of each input variable describing potential conditions in Tank AN-101 ($\rho_L$, H, and $[H_2]_{gas}$) were arranged in random orders
- the first entries from each list were grouped to form the first combination

- the second entries from each list were grouped to form the second combination
- the third entries from each list were grouped to form the third combination (and so on)
- the last entries from each list were grouped to form the 5000th combination.

In this way, all values from the representative distribution of $\rho_L$ were included in exactly one combination, all values from the representative distribution of H were included in exactly one combination, all values from the representative distribution of $[H_2]_{gas}$ were included in exactly one combination, and the 5,000 combinations were formed in a random fashion (and based on the assumption that $\rho_L$, H, and $[H_2]_{gas}$ were uncorrelated). The resulting 5,000 combinations of 3-tuples of $\rho_L$, H, and $[H_2]_{gas}$ were then used to calculate 5,000 simulated sediment depth values for Tank AN-101.

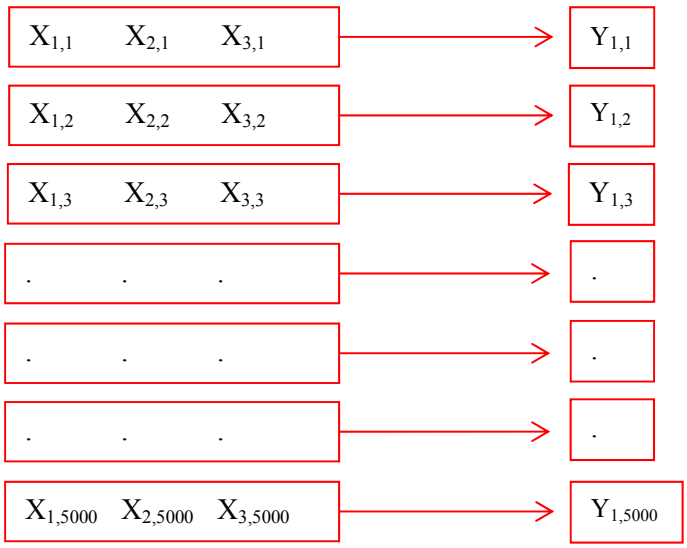


The same process was conducted relative to Tank AN-106. The resulting 5,000 sediment depth values for Tank AN-101 and the 5,000 sediment depth values for Tank AN-106 can be viewed as simulated distributions that provide preliminary insight (e.g., to estimate quantities such as average value and variation) concerning potential values of the limiting sediment depth for a specified LFL limit based on the flammability model for these two waste tanks.

## 3.2 Layer Densities

Difference in the sediment layer density, $\rho_S$, and liquid layer density, $\rho_L$, defines the neutral buoyancy gas fraction, i.e., the gas fraction required for the sediment to be buoyant in the overlaying supernatant liquid. As described in Stewart et al. (2005), allowing the sediment and liquid densities to vary indiscriminately and independently within their respective distributions will produce non-physical combinations with respect to neutral buoyancy, $\alpha_{NB}$, defined by

$$\alpha_{NB} = 1 - \frac{\rho_L}{\rho_S} \tag{3.1}$$

Given the dependency of the flammability model on the neutral buoyancy gas fraction, this result is clearly undesirable. Therefore, in addition to the obvious constraint that the supernatant liquid is less dense than the sediment, the sediment density must be correlated with the liquid density. Following Stewart et al. (2005), it is assumed that the interstitial liquid in the sediment is identical to the supernatant liquid. Thus, the sediment density, with consideration of the undissolved solids (UDS) properties and concentration, may be computed directly from the supernatant density. The in situ sediment is a solid-liquid-gas matrix. In its degassed state, the total mass is the sum of the liquid and solid masses. The sediment density may then be expressed as

$$\rho_S = \phi\rho_{UDS} + (1-\phi)\rho_L \tag{3.2}$$

where $\rho_{UDS}$ is the UDS density. The UDS densities for the projected retrieval states are determined from the tank average UDS densities based on the solid crystal phases proposed as present from Wells et al. (2011) volume weighted by the Table 3.1 values. The resultant UDS densities are 2,733 kg/m$^3$ for Tank AN-101 and 2,377 kg/m$^3$ for Tank AN-106. In Equation (3.2), $\phi$ is the UDS volume fraction in the sediment layer which can be computed for each of the respective projected retrieval tanks with UDS density (Wells et al. 2011), and median sediment and liquid densities (Yarbrough 2013) via

$$\phi = \frac{\rho_S - \rho_L}{\rho_{UDS} - \rho_L} \tag{3.3}$$

As for the UDS densities, the UDS volume fraction for the projected retrieval states are determined by volume weighting (Table 3.1) the respective computed individual tank values. The resultant UDS volume fractions for the projected retrieval states are 0.34 and 0.31 for Tanks AN-101 and AN-106, respectively.

The validity of using the methodology of Equation (3.2) and Equation (3.3) and the approximated UDS density and volume concentration values is evaluated with respect to the range of measured sediment values for the tanks in question as well as the computed neutral buoyant gas fraction. Meacham and Kirch (2013) used a liquid density of 1,170 kg/m$^3$ and sediment density of 1,660 kg/m$^3$ for Tank AN-101 and 1,080 kg/m$^3$ and 1,560 kg/m$^3$ for the respective layers in Tank AN-106.

Combining the liquid density values of Meacham and Kirch (2013) with the ranges of liquid density values for the respective C Tank Farm tanks (see Table 3.1) from Hu (2006), liquid density distributions for the projected retrievals were developed as shown in Figure 3.1 and Figure 3.2. The maximum and minimum values for the C Tank Farm tanks are set by waste type in Hu (2006), not by specific measurements of the liquid. The median liquid density values are 1,170 and 1,080 kg/m$^3$ for Tanks AN-101 and AN-106, respectively, and the maximum and minimum values for each tank are 1,227 and 1,000 kg/m$^3$ (Table 3.2).

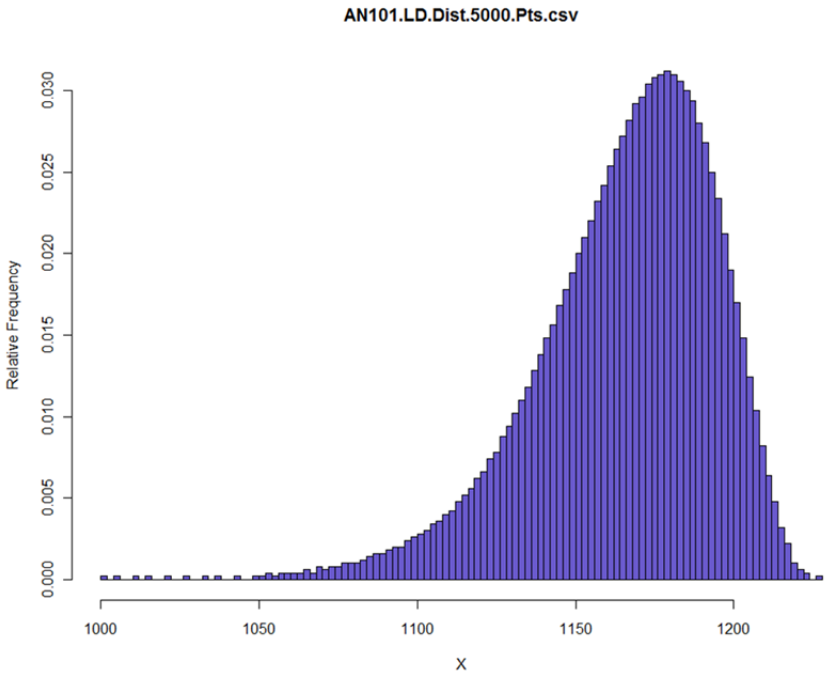


a)

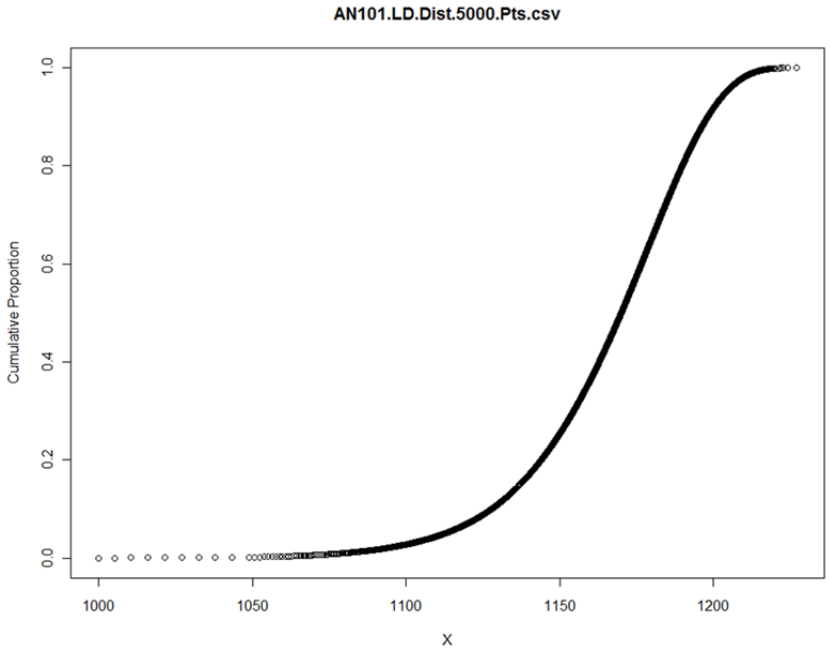


b)

**Figure 3.1**. Tank AN-101 Liquid Density Distribution (kg/m$^3$). a) probability distribution, b) cumulative distribution.

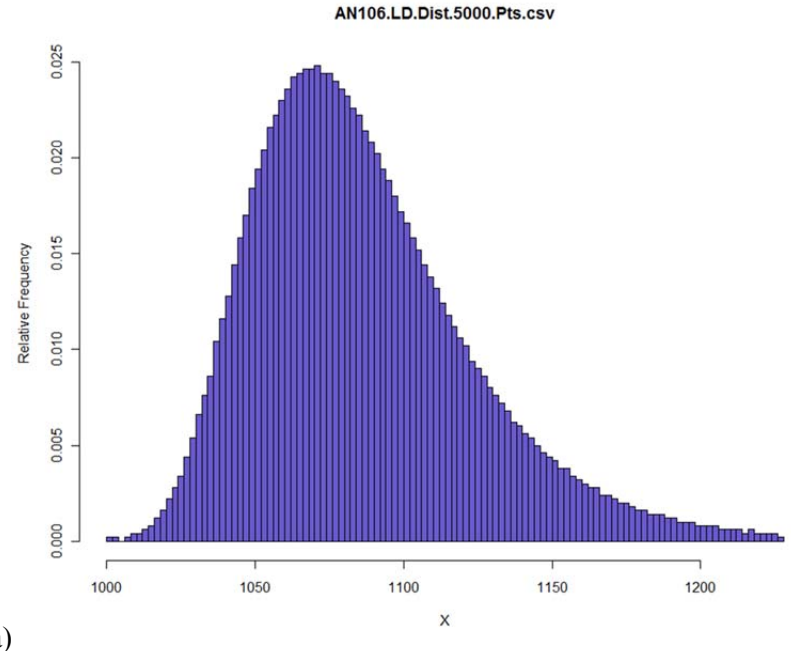


a)

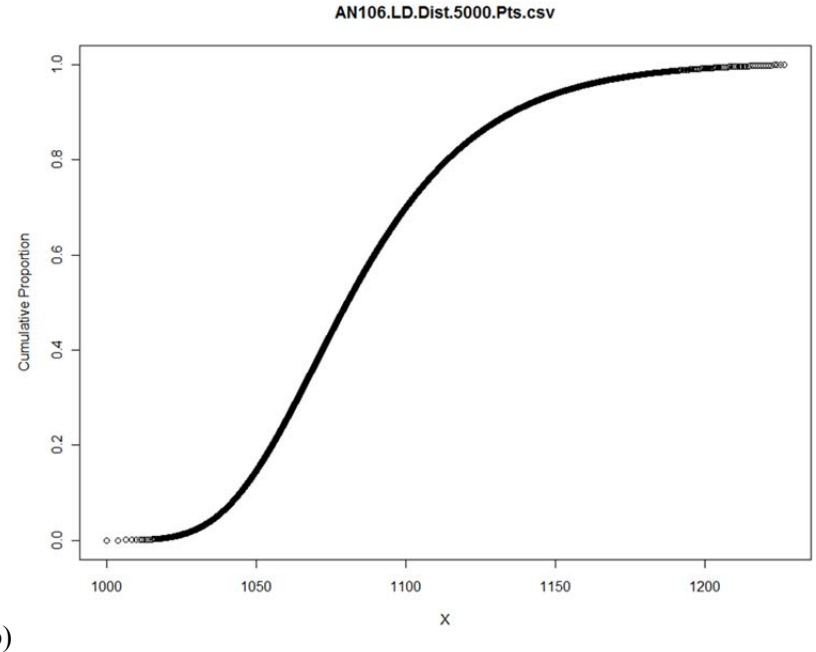


b)

**Figure 3.2**. Tank AN-106 Liquid Density Distribution (kg/m$^3$). a) probability distribution, b) cumulative distribution.

**Table 3.2**. Liquid Density Distributions (kg/m$^3$)

| Tank | Median | Maximum | Minimum | Distribution |
|---|---|---|---|---|
| AN-101 | 1,170 | 1,227 | 1,000 | Unimodal/Near-Gaussian |
| AN-106 | 1,080 | 1,227 | 1,000 | Unimodal/Near-Gaussian |

These liquid density distributions, together with the volume weighted UDS density and volume fraction values, yield the sediment density values via Equation (3.2) depicted as cumulative distributions in Figure 3.3. The Meacham and Kirch (2013) sediment density value for Tank AN-101, 1,660 kg/m$^3$, is at approximately the 5$^{th}$ percentile of the computed results. The Meacham and Kirch (2013) sediment density value for Tank AN-106, 1,560 kg/m$^3$, is at approximately the 90$^{th}$ percentile of the computed results. However, comparison to the range of measured values from Harrington (2013) is reasonable.

Two methods (based on sample data and waste type) of determining bulk sediment density layering in each C Tank Farm tank were used in Harrington (2013). The combined range of sediment bulk density in Tank AN-101 was determined as 1,400 kg/m$^3$ to 1,760 kg/m$^3$ and 1,230 kg/m$^3$ to 1,620 kg/m$^3$ in Tank AN-106. Shifting the lower calculated sediment densities of Figure 3.3 to reflect the minimum values (e.g., 1,580 kg/m$^3$ to 1,400 kg/m$^3$ in Tank AN-101) would require non-physical lower liquid density values (less than water) or lower solid density or solid volume fraction. Shifting the latter two parameters lower would of course decrease the upper end of the calculated sediment densities, which are currently in approximate agreement. Thus, in consideration of the acceptable calculated range of neutral buoyant gas fraction as discussed below, the described calculation methodology for the sediment density is employed.

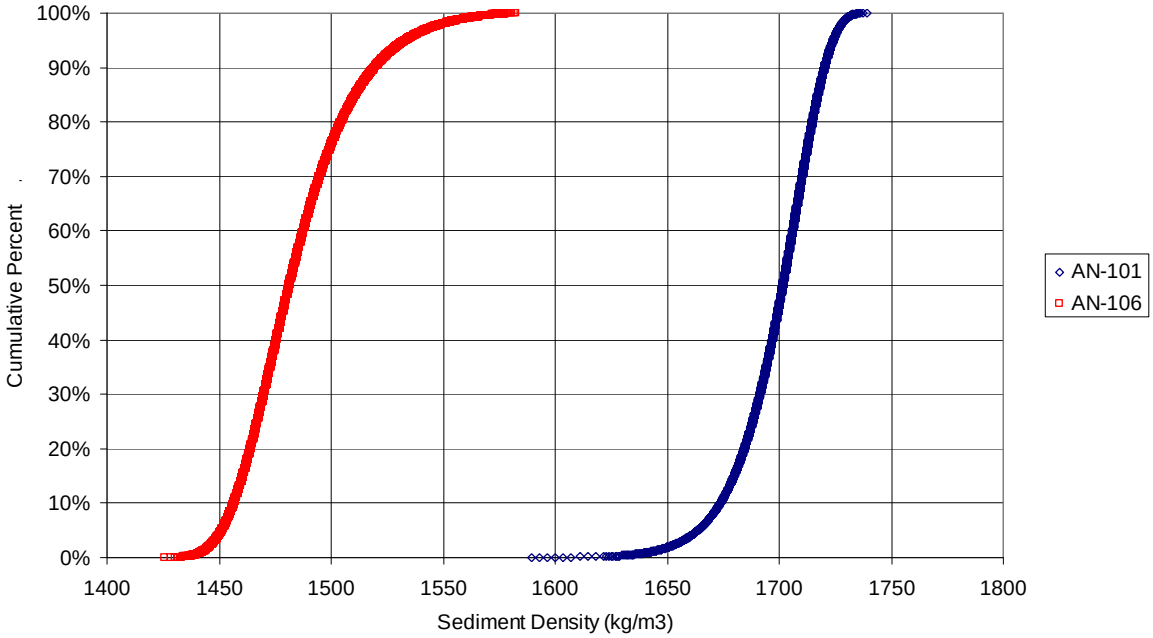


**Figure 3.3**. Calculated Sediment Density

Using the Meacham and Kirch (2013) layer density values in Equation (3.1), representative neutral buoyancy gas fractions for Tanks AN-101 and AN-106 are 0.30 and 0.31, respectively. Combining the respective liquid and sediment density inputs and results of Figure 3.1, Figure 3.2, and Figure 3.3 via Equation (3.1) results in the calculated neutral buoyancy gas fractions shown in Figure 3.4. As expected, similar percentiles are achieved between the Meacham and Kirch (2013) values and the calculated values of the sediment density. Of primary significance, however, is the difference in neutral buoyancy is on the order of 20% to 25%.

Stewart et al. (2005) directly compared the computed neutral buoyancy gas fraction to measured retained gas values for the BDGRE tanks. From the independent sediment and liquid density distributions, combinations that produced very low neutral buoyancy gas fraction would potentially preclude the observed gas release volumes or retained gas volume estimates from in situ measurements or waste surface level histories, while a high neutral buoyancy gas fraction would potentially exceed the estimated gas retention quantities. From the Tank AN-103 example of Stewart et al. (2005), computation of the neutral buoyant gas fraction indiscriminately using the data density distributions yields results ranging from approximately 0.02 to 0.27. These results under-predict the reported gas content in the sediment layer from Hedengren et al. (2000) by a factor of 6 and over-predict by a factor of 2.5, respectively. Conversely, with the sediment density computed via the process described here, the neutral buoyancy gas fraction ranged from approximately 0.10 to 0.14, which under- and over-predicted the retained gas content in Hedengren et al. (2000) by factors of 1.1 and 1.3, respectively.

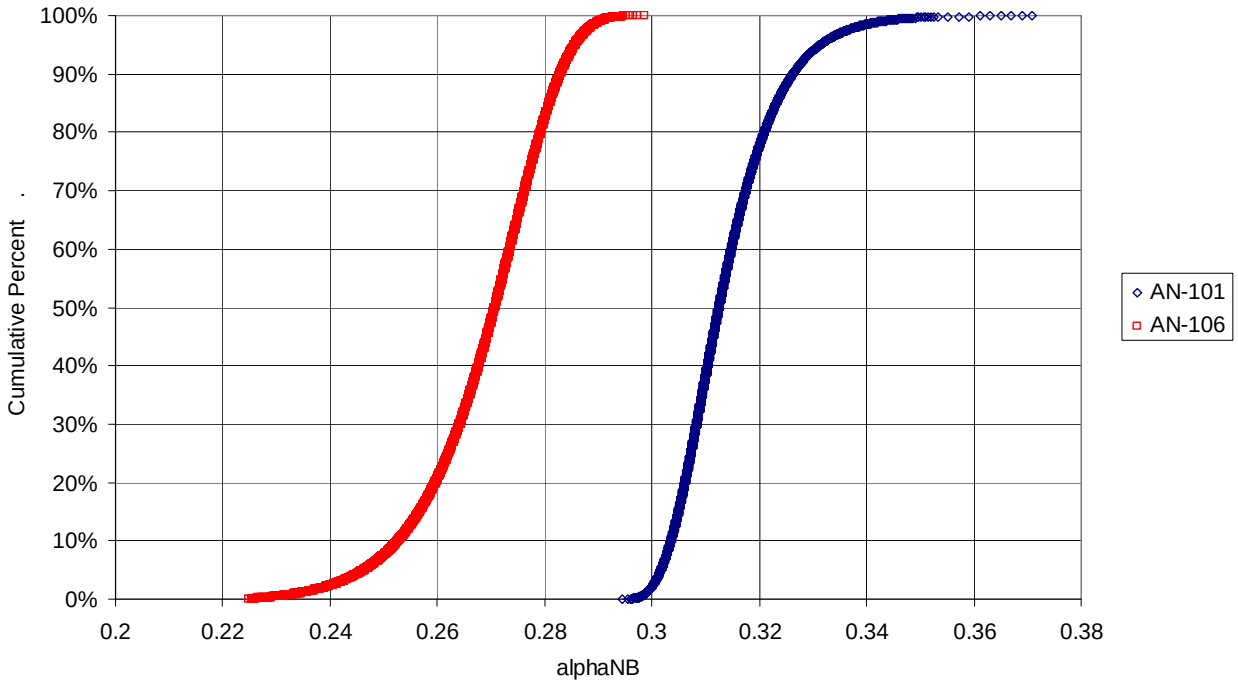


**Figure 3.4**. Calculated Neutral Buoyancy Gas Fraction

Therefore, with similar sediment density ranges to actual waste data and reasonable variation in the computed neutral buoyancy gas fraction relative to the Stewart et al. (2005) analysis, the liquid density for the flammability model analysis of Tanks AN-101 and AN-106 will be taken from the Figure 3.1 and Figure 3.2 distributions. The sediment density will be computed from Equation (3.2) with the respective single-value UDS densities and volume fractions.

## 3.3 Layer Depth and Temperature

The buoyancy ratio, Equation (2.1), is a function of the sediment layer depth and temperature as well as the average gas pressure in the sediment. The average gas pressure in the sediment is a function of both the sediment and liquid layer depths, Equation (2.2). As described, the purpose of this current work

is to predict a sediment layer depth limit via the Stewart et al. (2005) flammability model in order to prevent the headspace hydrogen concentration from a spontaneous GRE exceeding a specific fraction of the LFL. Thus, the sediment depth is the independent parameter, and the projected sediment depths in the AN Tank Farm tanks are only considered with respect to target depths and for the effect on the model applicability as noted in Section 2.2.

Stewart et al. (2005) discuss how the sediment depth may affect the applicability of the flammability model (Section 2.2). They note the aspect of sediment depth that might compromise application of the flammability model would be wall effects. In vessels much taller than their diameter, the wall effect would tend to amplify the influence of the sediment yield stress in shear and increase the excess buoyancy required for a gob to break free. However, they state with a DST tank diameter of 900 in. (75 ft), wall effects are minimal even at very high sediment depths. The small effect of increased hydrostatic pressure is included explicitly in the model.

The sediment depth of the largest BDGRE tank (the only tank with GREs that exceed the LFL, Hedengren et al. 2000), Tank SY-101, has been as high as 6 meters (236 in.) (Antoniak 1993). The upper bound of the 99% confidence interval for the sediment depth distribution listed for Tank SY-101 at 6.6 meters (260 in.) is suggested by Stewart et al. (2005) as a possible limit for the flammability model, further stating that "this result probably supports the application of…the flammability model to sediment layers up 7 meters (276 inches) in depth." The projected target sediment depths in Tanks AN-101 and AN-106 are approximately 7.8 meters (308 in.) and 5.7 meters (226 in.), respectively (Barton et al. 2013). Given 1) the lack of a specific basis to limit the flammability model to the 6.6-meter (260-in.) sediment depth, 2) the likely weak influence of depth because of wall effects relative to the DST diameter as described, 3) the approximately 10% increase to the projected 7.8-meter (308-in.) target in Tank AN-101 over the possible 7-meter (276-in.) limit, and 4) the squared dependence (most significant term) in the buoyancy ratio, the flammability model is not modified to account for the projected sediment depths.

The average sediment temperature in the projected AN Tank Farm tanks is taken as the average of the respective AN Tank Farm and C Tank Farm (see Table 3.2; volume weighting is not used) sediment temperatures from Yarbrough (2013): 299 K in Tank AN-101 and 298 K in Tank AN-106. These temperatures are approximately 5% lower than the average sediment temperatures in the BDGRE tanks (Stewart et al. 2005).

Uytioco (2011) provides supernatant liquid depth limits for Tanks AN-101 and AN-106 at projected retrieval conditions via the waste group flammability controls specified in Yarbrough (2013); specifically the energy ratio (see Section 1). Control of the GRE hazard by controlling the energy ratio assumes that a shallow supernatant layer will lead to a low energy ratio and, therefore, control the spontaneous GRE hazard. For the current analysis, the supernatant liquid depth is held constant at the Uytioco (2011) projected limiting depths of 2.1 and 2.5 meters (83 and 99 in.) in Tanks AN-101 and AN-106, respectively. This approach, following the Yarbrough (2013) methodology, keeps the energy ratio constant and therefore less than the control limit for GREs. Sediment depths predicted via the flammability model that exceed the projected target depth are not of significance. Varied waste layer densities that would impact the Uytioco (2011) limits are also not accounted for.

## 3.4 Gas Generation and Composition

The buoyancy ratio is a function of the total gas generation rate. In application, as described by Equation (2.1), the total generation rate is defined by the hydrogen gas generation rate and the concentration of hydrogen in the retained gas. The flammability model is also a function of the hydrogen concentration in the retained gas.

Distributions for the hydrogen gas generation rates are developed from the combination of the ranges of the hydrogen gas generation rates for the respective AN and C Tank Farm tanks (see Table 3.1) from Yarbrough (2013), and the projected completion-of-retrieval values from Uytioco (2011) as the medians. None of the tanks of interest have measured gas generation rate data, so the generation rates are calculated as described in these reference documents based on waste properties. The resultant distributions are shown in Figure 3.5 and Figure 3.6, and the distribution specifications are listed in Table 3.3. The hydrogen generation rate medians are within the same order of magnitude as the BDGRE tanks from Stewart et al. (2005).

Retained gas composition measurements are available for only a limited set of the Hanford waste tanks, and neither of the two specific AN Tank Farm tanks nor the C Tank Farm tanks have measured retained gas data (Mahoney 2000). The available hydrogen mole fraction range and distribution data are from salt slurry waste tanks. The radiolytic and chemical processes for hydrogen production do differ some between the high organic salt slurries and the lower organic waste sludges (Stock 2001) of Tanks AN-101 and AN-106. Studies on Savannah River sludges containing little organic (Hester 2002) showed that retained gas hydrogen concentrations ranged from only 0.08 to 0.32 volume fraction. In contrast, the distribution of the Hanford salt slurry hydrogen concentrations created from the Mahoney (2000) data range from 0.03 to 1 volume fraction (Figure 3.7). A roughly bimodal distribution is indicated, with generalized modes at approximately 0.30 and 0.65. Less than 0.1% of the distribution is less than the low organic sludge minimum value of 0.08. Using the Hanford Site saltcake hydrogen concentration data for estimating hydrogen concentration in the retained gas of Tanks AN-101 and AN-106 sludge waste is, therefore, likely conservative.

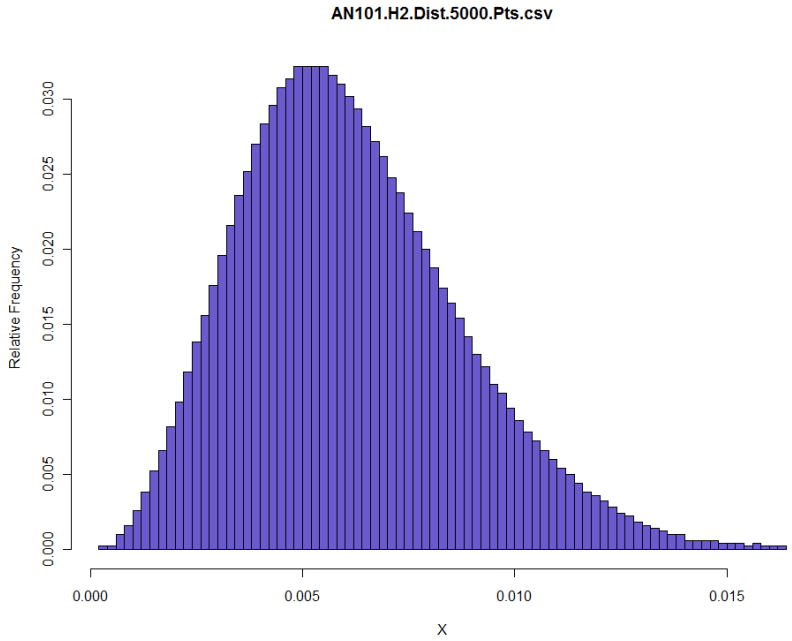


a)

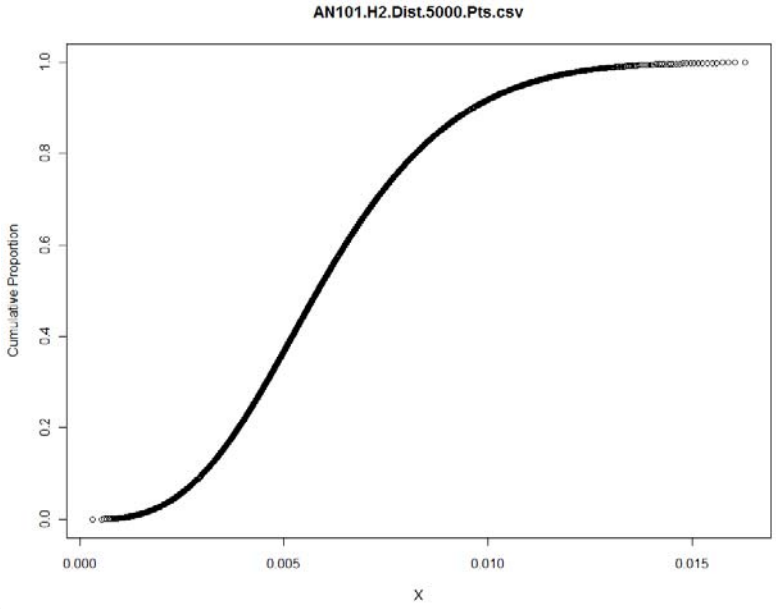


b)

**Figure 3.5**. Tank AN-101 Hydrogen Generation Rate Distribution (mols/$m^3$/day). a) probability distribution, b) cumulative distribution.

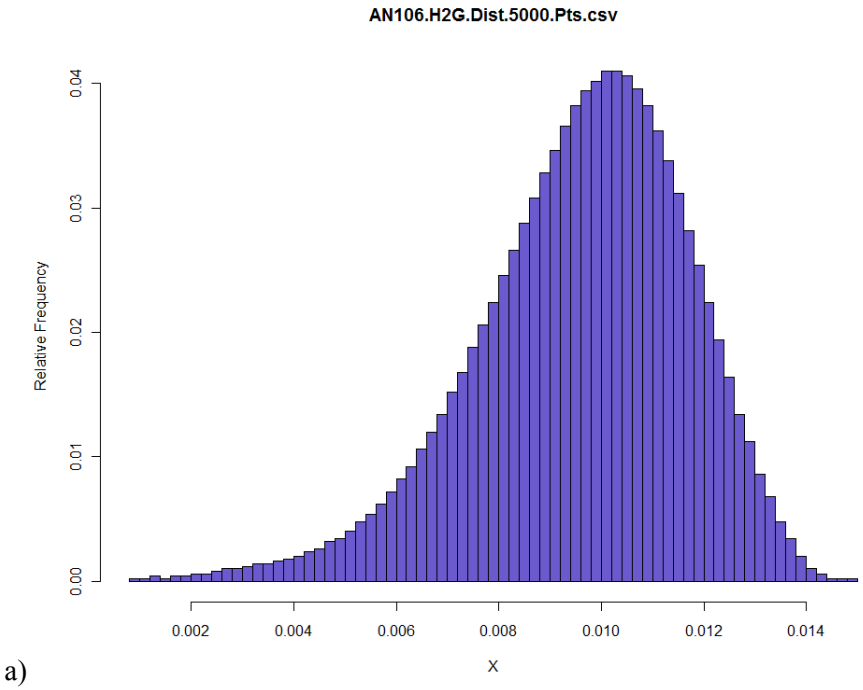


a)

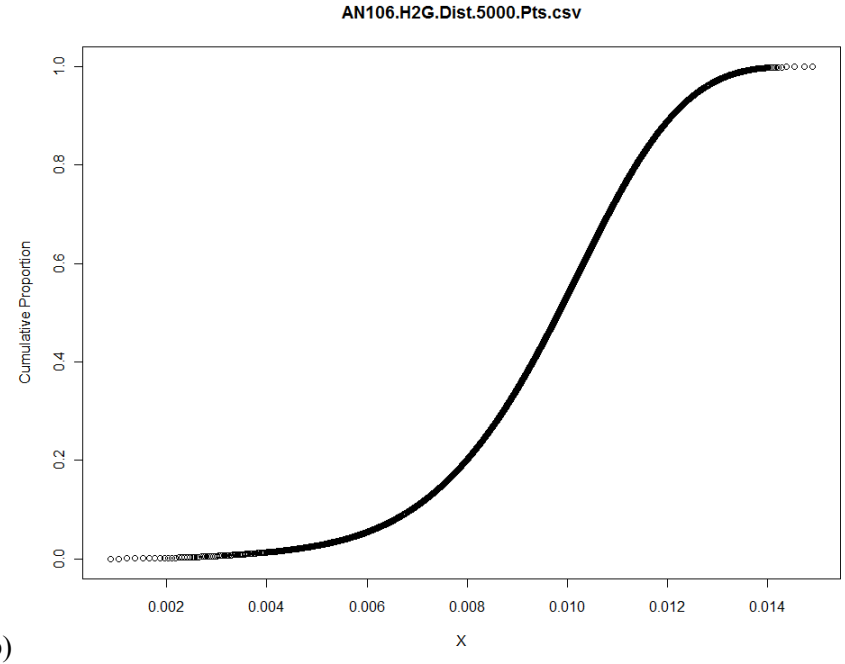


b)

**Figure 3.6**. Tank AN-106 Hydrogen Generation Rate Distribution (mols/$m^3$/day). a) probability distribution, b) cumulative distribution.

**Table 3.3**. Hydrogen Generation Rate Distributions (mols/$m^3$/day)

| Tank | Median | Maximum | Minimum | Distribution |
|---|---|---|---|---|
| AN-101 | 5.83E-03 | 1.63E-02 | 3.25E-04 | Unimodal/Near-Gaussian |
| AN-106 | 9.83E-03 | 1.49E-02 | 8.85E-04 | Unimodal/Near-Gaussian |

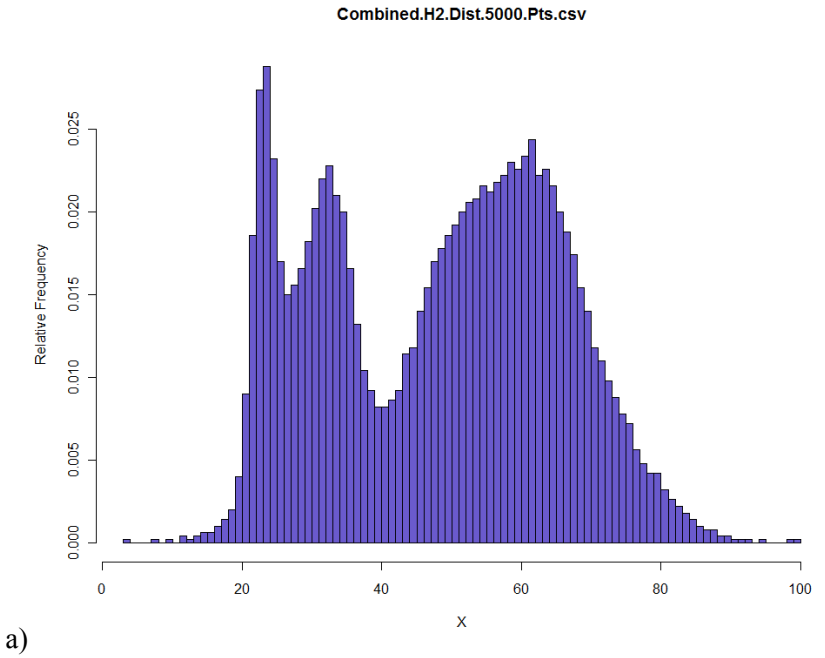


a)

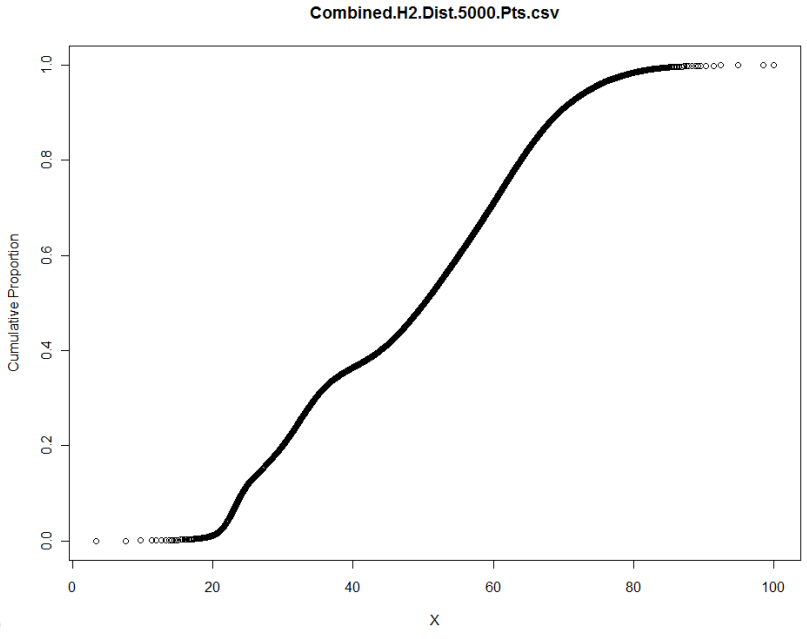


b)

**Figure 3.7**. Hydrogen Concentration in Retained Gas Distribution (volume fraction). a) probability distribution, b) cumulative distribution.

## 3.5 Sediment Rheology

The sediment rheology parameters that affect the flammability model (and the related BDGRE models) are discussed in detail in Stewart et al. (2005). Although there is no direct functionality of rheology in the flammability model except for unknown terms in the empirically adjusted coefficient of the buoyancy ratio, rheological properties of the sediment impact gas retention and release behavior,

therefore potentially impacting the applicability of the flammability model to the projected waste characteristics in the AN Tank Farm tanks with deep sludge sediments. In Section 3.5.1, a summary of the available data for estimating the specific parameters of interest of the retrieved tanks is provided, and the impacts of these characteristics to the flammability model relative to its databases are discussed.

## 3.5.1 Waste Rheology Data

The rheological characteristics of sediment that affect gas retention and release behavior as described by the BDGRE models include the yield stress in shear (shear strength) and whether the material is brittle or ductile as indicated by the strain at failure.

### 3.5.1.1 Shear Strength

As described in Wells et al. (2011), shear strength data generated through varied techniques are available for approximately 24% of the Hanford UDS inventory if a tank waste is treated as "represented" with respect to shear strength regardless of the number of measurements for a given tank. A sediment's shear strength depends on the characteristics of the system, including UDS concentration, particle size and distribution, particle shape, pH, quiescent time, elevation within the sediment, and retained gas content. Because of this dependence, the widely varied Hanford waste (widely varied with respect to particle size distribution, particle shape, etc.) has a broad range of shear strength values within the limited characterizations, and individual tanks may or may not have varied shear strength with sample location. Sediment shear strength data for the Hanford tank waste of the projected retrieval campaigns is, therefore, most relevant and data are available for five of the ten C Tank Farm tanks listed in Table 3.1.

Wells et al. (2011) provided cumulative sediment shear strength data by measurement technique wherein the probabilities were strictly based on measurement count. Consideration was given to improving this analysis via a reasonable statistical combination. However, it was determined that disparity between measurement techniques and results as well as incomplete waste characterization made meaningful combinations difficult (Gauglitz et al. 2009).

Shear-strength measurements summarized in Wells et al. (2011) are combined for Tanks C-104 (ten measurements), C-107 (13 measurements), C-110 ( two measurements), and single measurements from C-109 and C-112 into a single distribution. In this approach, measurement number, location, representativeness beyond initial sample conditions, the length of time the shear strength has developed, and the relative fraction of Hanford inventory are not accounted for, so the probability is strictly based on the number of measurements. All data are from ex-tank shear vane measurements on waste samples. The cumulative shear strength distribution for C Tank Farm sludge waste is provided in Figure 3.8. Maximum and minimum values of 7,826 and 75 Pa, respectively, are similar in magnitude to the range of measurements for all sludge wastes at Hanford (Wells et al. 2011). The median value is approximately 1,120 Pa, which corresponds with the representative value (1,000 Pa) used by Meacham (2010) for "high shear strength" waste.

The data presented in Figure 3.8 is used to represent the projected shear strength of the as-retrieved sediment in Tanks AN-101 and AN-106. Potential effects of retrieval, including chemical interaction of the individual tank wastes in the receipt AN Tank Farm tank, impacts to the particle size distribution

resulting from the sluicing and transfer process, settling and compaction influences on UDS concentration, etc., are not addressed.

A fundamental assumption of the buoyancy ratio model is that the shear strength increases linearly with depth (Section 2). The preponderance of evidence from Wells et al. (2011) for the limited characterizations of sludge waste indicates that the shear strength increases linearly with depth, although there is one well-characterized example of uniform shear strength (Tank AY-102). The only C Tank Farm tank with shear strength as a function of sediment depth is Tank C-104; the lowest measurement is near the top of the sediment, the highest measurement is near the bottom.

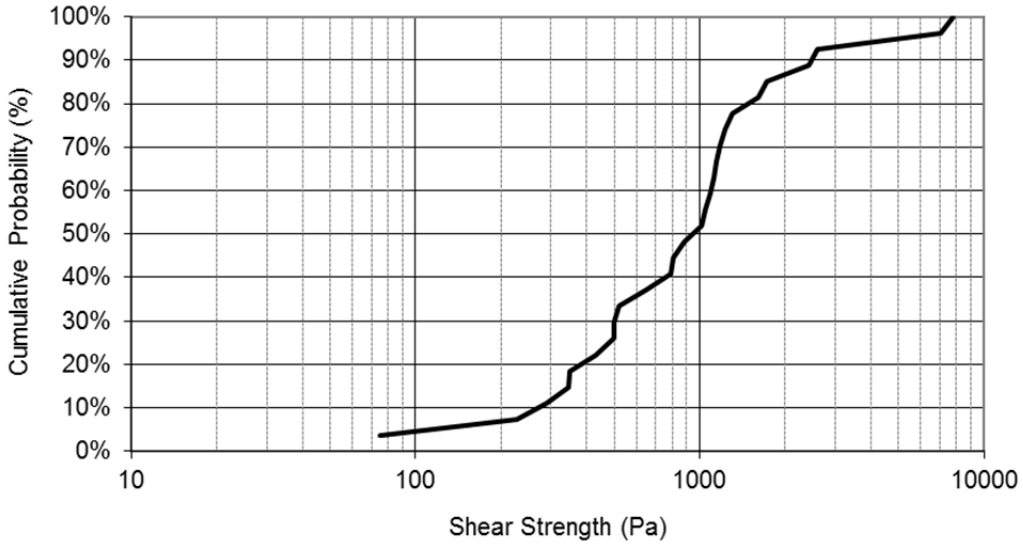


**Figure 3.8**. Data Summary of C Tank Farm Shear Vane Shear Strength

#### 3.5.1.2 Strain at Failure

The energy ratio criteria (Stewart et al. 1996; Meyer et al. 1997), referenced in Section 1, relates the potential energy released by a buoyant region of sediment rising through the supernatant liquid layer to the energy required to yield that region. The approximate expression for this latter energy includes the strain at failure. For the saltcake wastes in the BDGRE tanks, the strain at failure is estimated from stress-strain data for bentonite clay simulant at similar yield stress in shear values to the tank waste (Meyer et al. 1997). The strain at failure was an average of approximately 1.4 depending on the shear rate (see Figure 3.9) (Stewart et al. 1996; Meyer et al. 1997).

Gauglitz and Aikin (1997) selected bentonite clay as a waste simulant to represent the plastic, drooping behavior observed for samples of the saltcake BDGRE tanks (upon core sample horizontal extrusion). The necking behavior of the bentonite simulant is indicative of a ductile material. Conversely, sludge wastes exhibit more of a brittle fracture (Stewart et al. 2005).

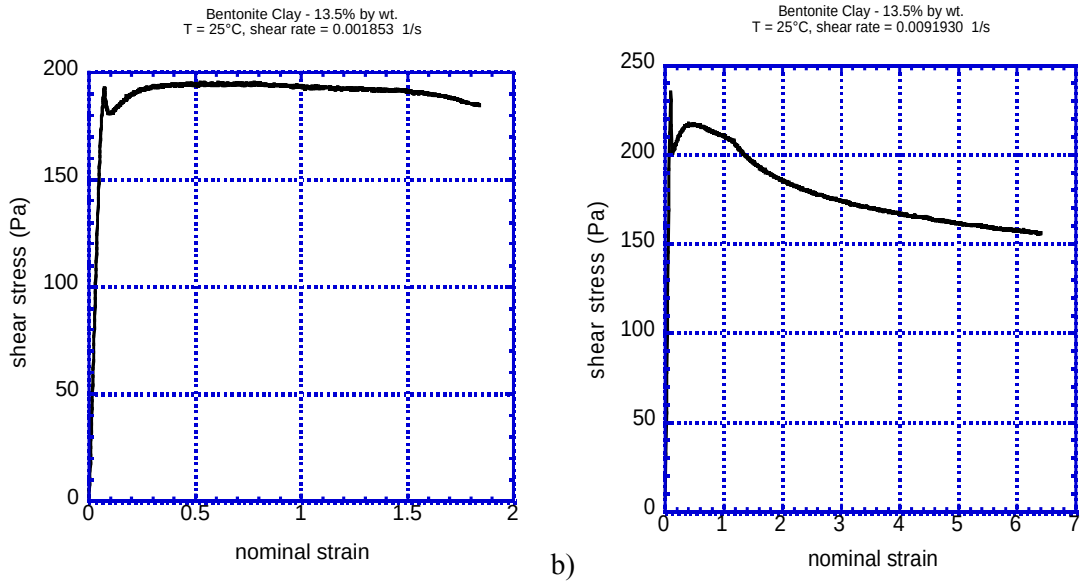


**Figure 3.9**. Stress-Strain for Bentonite Clay (Stewart et al. 1996). a) 190 Pa, shear rate 0.001853 (1/s), strain at failure ~1.6, b) 230 Pa, shear rate 0.0091930 (1/s), strain at failure ~1.2.

No actual waste data are available for the strain at failure. However, for sludge waste, Wells et al. (2010a) selected and developed chemical simulants to represent general sludge properties (simulant "S1") as well as the combination of the waste in Tanks C-104, C-111, and C-112 into Tank AN-101 (simulant "S2"). Characterization of these simulants in Wells et al. (2010b) provides shear vane data that can be converted to stress-strain data from which the strain at failure can be approximated similar to the bentonite clay simulant. The shear vane data includes time, stress, and vane rotation rate. The nominal strain corresponding to a given stress can be estimated from the vane rotation rate and time as

$$\text{Nominal\_Strain} = \omega t \tag{3.4}$$

where $\omega$ is the vane rotation rate (rad/s) and t is the test time (s).[1] An example stress-strain curve for the S2 simulant with a shear strength of approximately 2,000 Pa is shown in Figure 3.10, and the strain at failure can be estimated to be approximately 0.28. At this nominal strain, the relatively flat inelastic or plastic behavior appears to change with a sudden failure or relaxation. Estimated strain at failure for a range of simulant shear strengths from Wells et al. (2010b) is provided in Figure 3.11. As for the saltcake BDGRE tanks (e.g., Yarbrough [2013]), simulant estimates are used in this study for the strain at failure of the projected AN Tank Farm tank sludge sediments.

[1] Nominal strain for deformation due to a shear force is expressed as the angle in radians (e.g., Stevens 1979); for the shear vane data, the angle a vane blade has traveled in time t. It is not clear from the references how the bentonite clay data was evaluated.

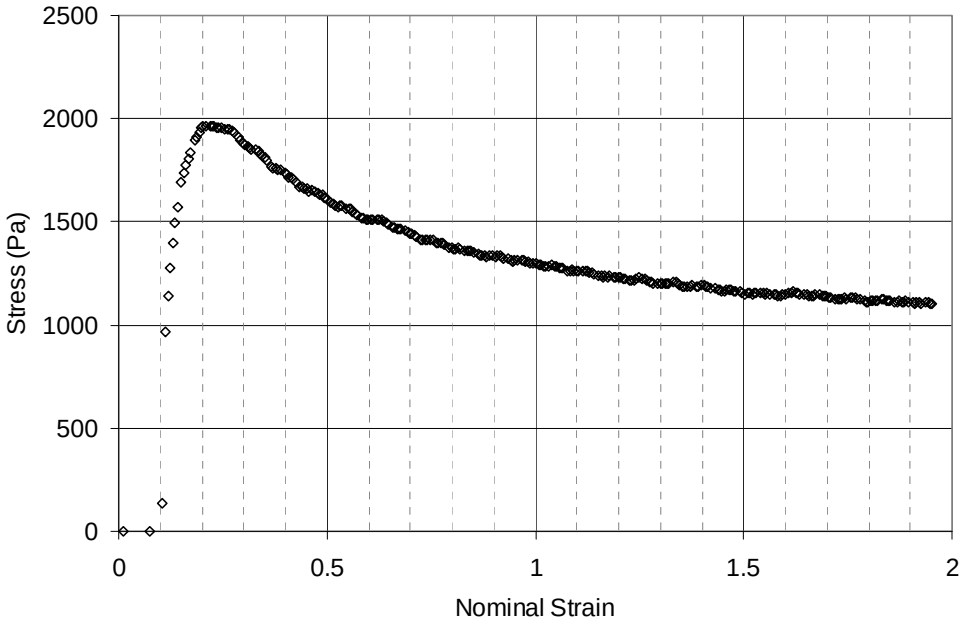


**Figure 3.10**. Stress-Strain for Chemical Simulant S2

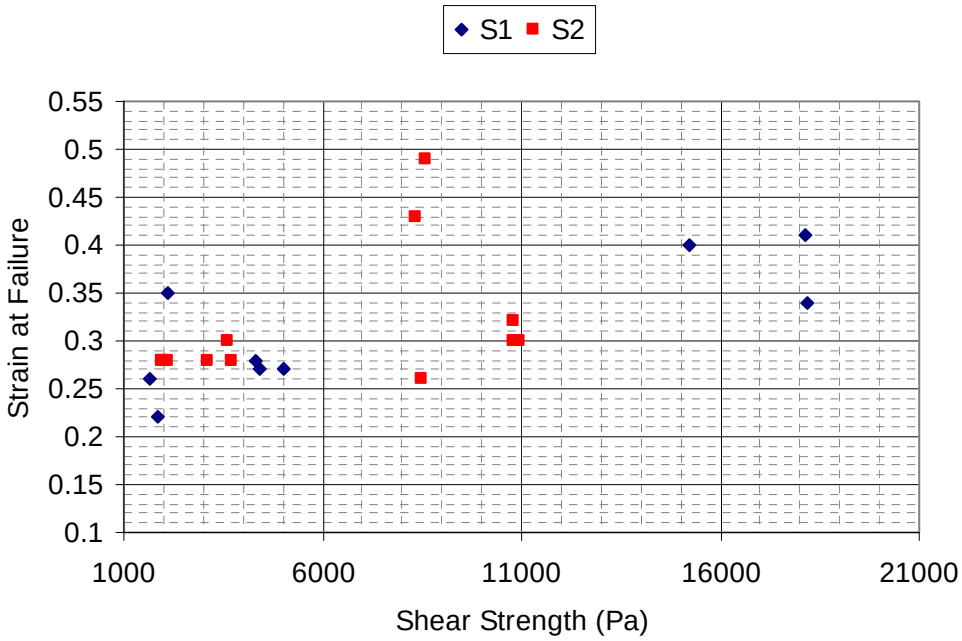


**Figure 3.11**. Chemical Simulants Strain at Failure

### 3.5.2 Effect of Waste Rheology on Flammability Model

Stewart et al. (2005) discusses how the rheological properties of sediment depth may affect the applicability of the flammability model, listed in Section 2.2 as:

- uniform sediment yield stress in shear with depth; the yield stress in shear or shear strength increases approximately linearly with depth in the BDGRE tanks, and this is a key assumption in the buoyancy ratio model
- strong sediment; the yield stress in shear, or shear strength, is greater than measured for the BDGRE tanks
- brittle sediment; the strain at failure is less than that postulated for the BDGRE tanks.

These waste characteristic differences may require adjustment of the flammability model. Based on the expected retrieved waste rheological characteristics defined in Section 3.5.1, determination is made whether model adjustments are required.

#### 3.5.2.1 Uniform Sediment Yield Stress in Shear with Depth

Based on the preponderance of evidence from Wells et al. (2011) for the limited characterizations of sludge waste, the shear strength increases linearly with depth in sludge wastes. With respect to the single example of uniform shear strength, Tank AY-102, Stewart et al. (2005) state:

> "Because the linear gas volume fraction profile in tanks with a uniform yield stress demands much smaller BDGREs than from a parabolic profile, a buoyancy ratio of 1.0 would be even more conservative for these tanks in terms of the size of the release."

and

> "However, it is neither important nor useful to plan operations … to prevent the inconsequential BDGREs resulting from a uniform yield stress. The flammability model provides a more meaningful limit. … Therefore, by considering the conservatism of the flammability model, it is clear that the buoyancy ratio model and criterion ensures that no hazardous releases will occur in sediment with uniform yield stress, though small BDGREs will occur at BR <1."

Thus, for the current evaluation to determine the allowed depth of sludge in Tanks AN-101 and AN-106 that will limit headspace hydrogen concentrations to a given fraction of the LFL, no modification is made to the flammability model to account for the potential of uniform sediment yield stress in shear with depth.

#### 3.5.2.2 Strong and Brittle Sediment

The shear strength measurements of C Tank Farm tank waste and, thus, the projected retrieval conditions in Tanks AN-101 and AN-106, can be up to a factor of 100 times greater than the values used for the BDGRE tanks (7,826 Pa maximum, Section 3.5.1.1, and 81 Pa, average in Tank AN-104, Meyer

et al. 1997). Thus, the retrieved sludge may be significantly stronger than the saltcake of the BDGRE tanks, which are the basis of the flammability model.

Materials that exhibit very little inelastic deformation (see discussion of Figure 3.9) can be classified as brittle, while other materials that undergo comparatively large inelastic deformations can be called ductile. With the amount of inelastic or plastic strain represented by the strain at failure (similar nominal strains at peak stress are observed for the bentonite clay, Figure 3.9, and the chemical simulants, e.g., Figure 3.10), the sludge is brittle in comparison to the BDGRE saltcake. The median strain at failure used for the sludge from Figure 3.11 is 0.28, which is five times less than the 1.4 used for the saltcake (Section 3.5.1.2).

The impact of this higher shear strength and lower strain at failure of the sludge with respect to the flammability model basis is evaluated using these specific parameters in the BDGRE models of the buoyancy ratio and energy ratio following Stewart et al. (2005). It is significant to use these models to evaluate the flammability model as the large GREs that form the flammability model basis are BDGREs.

Shear strength is indirectly included in the flammability model as an unknown term in the empirically adjusted calibration factor of the buoyancy ratio (Section 2.1). Specifically, the calibration factor has the slope of the yield stress in shear (shear strength) as a function of sediment depth, $m_\tau$. As referenced in Section 1, the DSA controls also include the energy ratio (ER) model, which is written in Yarbrough (2013) as

$$ER = \frac{\alpha_{NB}\gamma P_A}{(1-\alpha_{NB})\tau\varepsilon}\left[\left(1+\frac{1}{\gamma}\right)\ln(1+\gamma)-1\right] \tag{3.5}$$

where the non-dimensional pressure head $\gamma = \rho_L g H_L / P_A$, $\tau$ is the sediment shear strength (Pa), and $\varepsilon$ is the strain at failure. The energy ratio, therefore, is inversely proportional to both the shear strength and strain at failure.

Stewart et al. (2005) concluded, with respect to strong ductile sediments, that the buoyancy ratio, as a direct input to the flammability model (Equation (2.3)) should be corrected by the ratio of $m_\tau$ (change in shear strength over the sediment depth) for the strong sediment to $m_\tau$ for the BDGRE tanks:

$$BR_{strong} = BR_{[Eq.2.1]}\frac{[\Delta\tau/H_S]_{strong}}{[\Delta\tau/H_S]_{BDGRE}} \tag{3.6}$$

where $BR_{[Eq.\ 2.1]}$ is the buoyancy ratio computed with Equation (2.1). Stewart et al. (2005) used 130 Pa/m for the BDGRE tank's $m_\tau$. Therefore, any strong sediment with $m_\tau$ >130 Pa/m would have an increased buoyancy ratio via Equation (3.6), and this would result in a higher peak headspace hydrogen concentration from the flammability model (Equation (2.3)).

Stewart et al. (2005) stated that the energy ratio does not provide useful information on the potential for gas release in brittle sediments; a large gas release should be assumed from BDGREs in brittle sediments unless the depth of supernatant liquid is truly minimal. Therefore, based on Stewart et al. (2005), it can be concluded for strong and brittle sediments that the flammability model must be modified

via Equation (3.6), but this result may still underestimate the potential GRE size. These conclusions are evaluated for the specific sediment characteristics projected for Tanks AN-101 and AN-106.

The sediment shear strength distribution used to represent the projected sludge retrieval (Figure 3.8) is comprised of 27 individual measurements. From these 27 measurements, there are 350 unique pairs of measurements with positive differences (two of the 27 measurements are identical). If these differences are taken to represent the potential difference in a linearly increasing shear strength from the top to the bottom of the retrieved sediment, 350 values of $m_\tau$ can be calculated using an assumed sediment depth of 7.8 meters (308 in.) (Section 3.3).

For the BDGRE tanks, the in situ yield stress in shear measurements can be specifically evaluated. However, all of the BDGRE tanks with this yield stress data have a so-called "stationary layer" (Meyer et al. 1997), so the measured yield stress values start at the top of the sediment and extend to the "stationary layer" (see also Hedengren et al. 2000). This lowest-depth measurement can be denoted as the maximum measured value. Beyond the point at which the yield stress measurements stops, the shear strength is at least 900 Pa. Two distributions (based solely on measurement count; sediment depths taken per the yield stress measurement elevations from Meyer et al. 1997 and Hedengren et al. 2000) for the $m_\tau$ of the BDGRE tanks are thus created: 1) top of sediment to maximum measured value depth, "BDGRE Tanks to Max Measured," and 2) top of sediment to just below the maximum measured value depth at 900 Pa, "BDGRE Tanks to 900 Pa." The latter case is significant as the measured linear gas fraction profiles with sediment depth in the BDGRE tanks (Meyer et al. 1997; Hedengren et al. 2000) result in the entire sediment depth being buoyant at sufficient average void (Wells et al. 2002; Stewart et al. 2005). Further, the 900 Pa is an estimate of the minimum shear strength required to stop the measurement device; the shear strength can potentially be greater than 900 Pa. Ex-tank shear strength estimates from core extrusion video were in relatively close agreement with the Meyer et al. (1997) in situ measurements but had higher results (up to ~3,300 Pa) than 900 Pa at the lower sediment depths (Gauglitz and Aikin 1997; Rassat et al. 2003).

The projected sludge and BDGRE tank distributions for $m_\tau$ are shown in Figure 3.12. Only approximately 10% of the projected sludge $m_\tau$ results exceed the BDGRE tank estimates. Higher $m_\tau$ values would be achieved for the BDGRE tanks if the higher ex-tank shear strength estimates were included in the evaluation. It is judged that there is low probability that the $m_\tau$ of the projected sludge will exceed the $m_\tau$ of the BDGRE tanks which form the basis of the flammability model.

Stewart et al. (2005) made their arguments that a large gas release should be assumed from BDGREs in brittle sediments based on the reduced strain at failure and the energy ratio, Equation (3.5); the energy required to yield the buoyant sediment would be much less for the brittle material. However, this is true only for relatively weak materials. The energy required to yield the sediment is expressed in Meyer et al. (1997) as

$$E_Y = V_S \tau \varepsilon \tag{3.7}$$

where $V_S$ is the buoyant sediment volume, and the product of the shear strength and strain at failure in Equation (3.7) provides part of the denominator for the energy ratio (Equation (3.5)). Thus, the energy ratio and, therefore, the gas release, will be larger than the BDGRE tanks only if this product, $\tau\varepsilon$, is less than the BDGRE tank values.

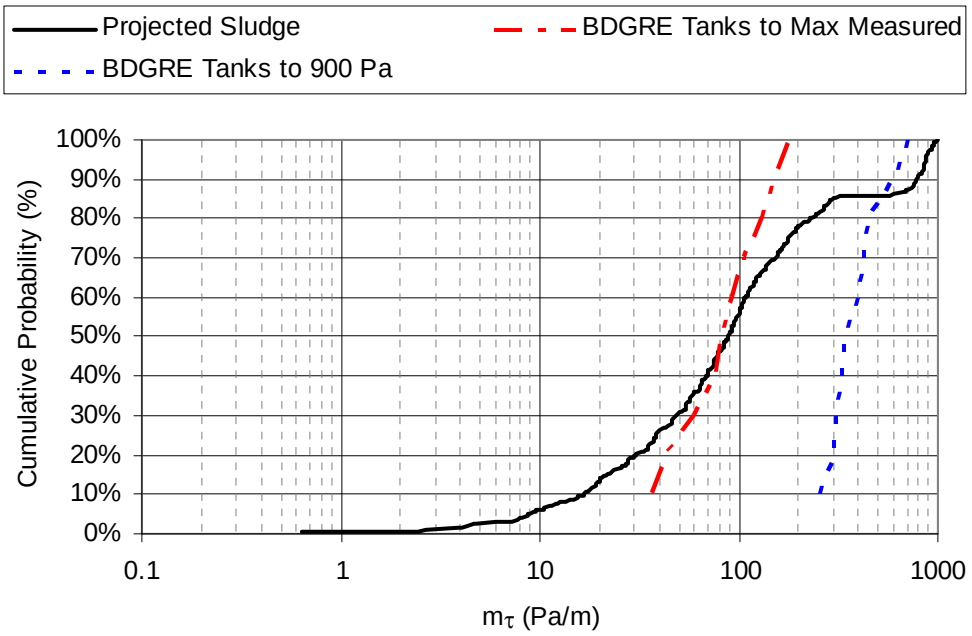


**Figure 3.12**. Comparison of Projected Sludge and BDGRE Tanks $m_\tau$

The average shear strength for the 350 projected sludge $m_\tau$ values of Figure 3.12 can be combined with the median strain at failure from Figure 3.11, 0.28, to provide 350 projected sludge $\tau\varepsilon$ values. Similarly, $\tau\varepsilon$ values can be computed for the BDGRE tanks using the average shear strength values of Meyer et al. (1997) and the average strain at failure of 1.4 (Section 3.5.1.2). In Figure 3.13, the computed $\tau\varepsilon$ values are plotted together with the $m_\tau$ values of Figure 3.12. To have larger GREs in strong, brittle sludge:

$$[m_\tau]_{sludge} > [m_\tau]_{BDGRE} \quad \text{and} \quad [\tau\varepsilon]_{sludge} < [\tau\varepsilon]_{BDGRE}$$

where the subscript sludge refers to the projected sludge values and the subscript BDGRE refers to the values for the BDGRE tanks that form the flammability model basis. The $m_\tau$ criterion is depicted with the orange (for "BDGRE Tanks to Max Measured") and red (for "BDGRE Tanks to 900 Pa") shaded areas, and the $\tau\varepsilon$ criterion is depicted in the yellow shaded area (Figure 3.13). As for the $m_\tau$ shown in Figure 3.12, there are very limited $\tau\varepsilon$ cases for the projected sludge that would result in larger GREs. More significant is that there are no projected sludge values in the boxed area of "Larger GREs," which is the convergence of the two criteria, even with the more conservative "BDGRE Tanks to Max Measured" values (convergence of the orange and yellow shaded areas, Figure 3.13). Therefore, it is concluded that no adjustments need to be made to the flammability model to account for the projected rheology of the sludge retrieved into Tanks AN-101 and AN-106.

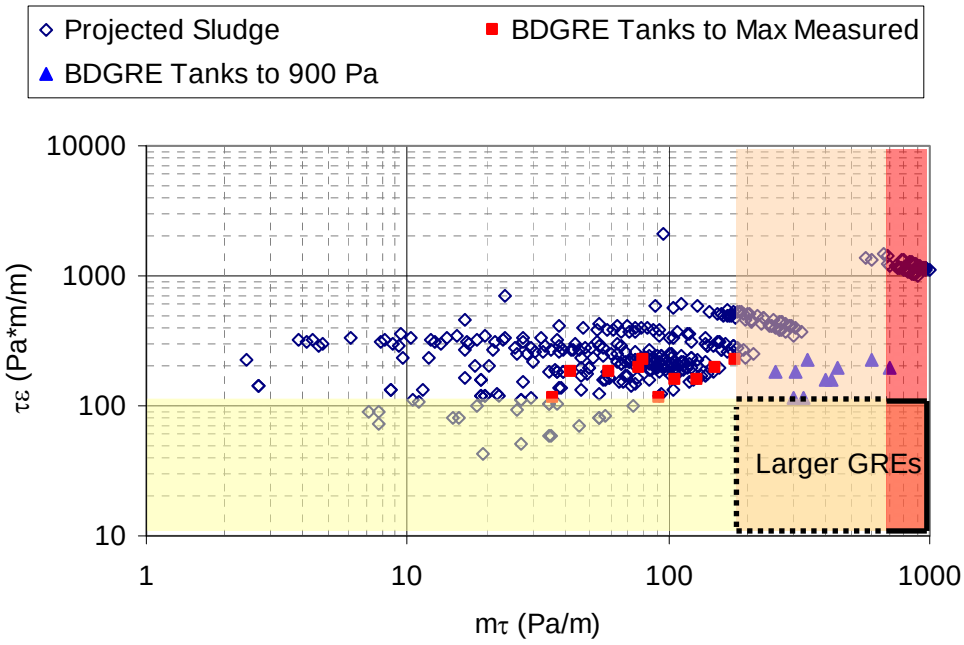


**Figure 3.13**. Comparison of Projected Sludge and BDGRE Tanks $m_\tau$ and $\tau\varepsilon$

# 4.0 Results

The Stewart et al. (2005) flammability model (Section 2.1) is applied to the projected characteristics of sludge sediment retrieved from C Farm tanks into AN Farm tanks AN-101 and AN-106 (Section 3). A Monte Carlo simulation approach is used (Section 3.1), and for each combination of input parameters, the sediment height that will limit headspace hydrogen concentrations to a given fraction of the LFL is determined. The buoyancy ratio is calculated from Equation (2.4), the flammability model, which provides a buoyancy ratio such that the headspace hydrogen concentration is limited to the specified fraction of the LFL. The buoyancy ratio is also calculated from Equation (2.1), and the sediment height is adjusted such that the buoyancy ratio calculated from both Equation (2.4) and Equation (2.1) is equivalent. This sediment height is, therefore, the limiting depth for a specified LFL limit based on the flammability model.

The results are presented by first addressing the effect of the simulation approach, and then evaluating the effect of specific parameters. With these bases established, the implications of specific results are discussed. In Section 4.1, the effect of the simulation approach with respect to the Monte Carlo methodology is addressed. Parameter sensitivities are investigated in Section 4.2. Discussion of the results and implications is made in Section 4.3.

## 4.1 Effect of Simulation Approach

The Monte Carlo simulation described in Section 3.1 was run five times. That is, the random sampling of 5,000 combinations of $\rho_L$, H, and $[H_2]_{gas}$ from the domain of $1.25 \times 10^{11}$ such combinations available for determining sediment depth (as it relates to the flammability model) for Tank AN-101 was conducted five times, thereby generating five sets of 5,000 simulated sediment depths for Tank AN-101. Similarly, five sets of 5,000 simulated sediment depths were generated for Tank AN-106.

The five sets of 5,000 sediment depths for Tank AN-101 do not cover all possible combinations of input variables (i.e., crossing all values for the input variables $\rho_L$, H, and $[H_2]_{gas}$) in the domain for Tank AN-101. Similarly, the five sets of 5,000 sediment depths for Tank AN-106 do not cover all possible combinations of input variables in the domain for Tank AN-106. As mentioned in Section 3.1, sediment depth would need to be determined for all $1.25 \times 10^{11}$ combinations of $\rho_L$, H, and $[H_2]_{gas}$ for both Tanks AN-101 and AN-106 in order to cover the full domains defined by the representative distributions used to describe of $\rho_L$, H, and $[H_2]_{gas}$. However, the five sets of results do provide a greater view of the respective domains than a single run of the Monte Carlo simulation for each waste tank. Furthermore, all of the representative values of each input variable are included in one combination of input variables used to generate the simulated sediment depths. Other random selection strategies that could have been used for the Monte Carlo simulation might not have ensured that all representative values of each input variable were included in the generation of simulated sediment depths, thereby resulting in potential under-representation of less typical input variable values.

The five Monte Carlo simulations for the respective tanks were equivalent for the bulk of the simulated sediment depth distributions and only had slight differences in the tails (i.e., <<than the 1st percentile, >than the 99th percentile). Therefore, a simulation approach using 5,000 combinations was deemed to adequately represent the flammability model predicted sediment depths.

## 4.2 Parameter Sensitivity

The effects of the hydrogen concentration in the retained gas and the headspace flammability limit on the calculated limiting sediment depth are evaluated in the following subsections.

### 4.2.1 Effect of Hydrogen Concentration in the Retained Gas

As described in Section 3, the parameter with significant uncertainty relative to the projected sludge waste is the hydrogen fraction in the retained gas. There are no measurements for the tanks in question, nor are there measurements for any Hanford sludge wastes. Comparison to studies on Savannah River sludges indicated that using the Hanford Site saltcake hydrogen concentration data for estimating hydrogen concentration in the retained gas of Tanks AN-101 and AN-106 sludge waste would most likely be conservative (Section 3.4). However, the effect of the application of the hydrogen concentration data from the saltcake tanks is evaluated.

Sediment depths that limit the hydrogen concentration in the headspace to 60% of the LFL (see Section 4.2.2) are computed through the Monte Carlo parameter values for three H2 Cases: 1) the distribution created from the saltcake-measured hydrogen concentration (Figure 3.7); 2) the approximate lower mode of Figure 3.7, 0.30; and 3) the approximate upper mode of Figure 3.7, 0.65.

The limiting sediment depths for H2 Case 1 are shown in Figure 4.1, H2 Case 2 in Figure 4.2, and H2 Case 3 in Figure 4.3. For each figure, the symbols denote the sediment depth results for Tanks AN-101 and AN-106, respectively, and the cumulative distributions are the 5,000 Monte Carlo simulation results. The vertical dashed lines indicate the projected target sediment depths of approximately 7.8 meters (308 in.) in Tank AN-101 and 5.7 meters (226 in.) for Tank AN-106 (Barton et al. 2013), and the vertical span of these target depths has no meaning with respect to the cumulative distribution. For comparison, consider the $50^{th}$ percentile results for each figure relative to the target sediment depth for Tank AN-106 (red square symbols and red dashed line, respectively). For H2 Case 1, the $50^{th}$ percentile is to the left of the target sediment depth; for H2 Case 2, they almost coincide; and for H2 Case 3, the $50^{th}$ percentile is further to the left of the target sediment depth than for H2 Case 1. As expected, higher allowable sediment depths are achieved with the hydrogen fraction fixed at 0.30 (H2 Case 2), and H2 Case 3 is the most limiting. Obviously, assuming that the retained gas is 100% hydrogen would be even more conservative, but with the sediment target depths for the H2 Case 3, 0.65 hydrogen concentration already exceeding well over 90% of the simulation results for both Tanks AN-101 and AN-106, there is no reason to evaluate the 100% hydrogen case. As previously stated, using the Hanford Site saltcake hydrogen concentration data for estimating hydrogen concentration in the retained gas of Tanks AN-101 and AN-106 sludge waste is likely conservative and has some basis with respect to actual waste data.

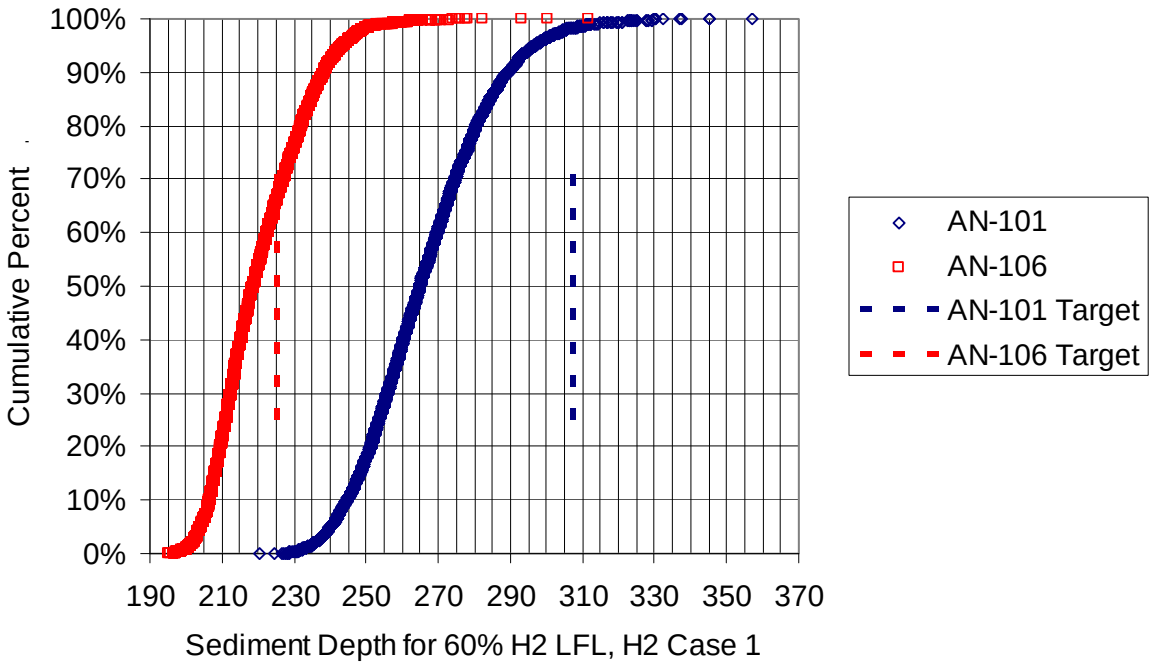


**Figure 4.1**. H2 Case 1 (LFL Case 1, see Section 4.2.2)

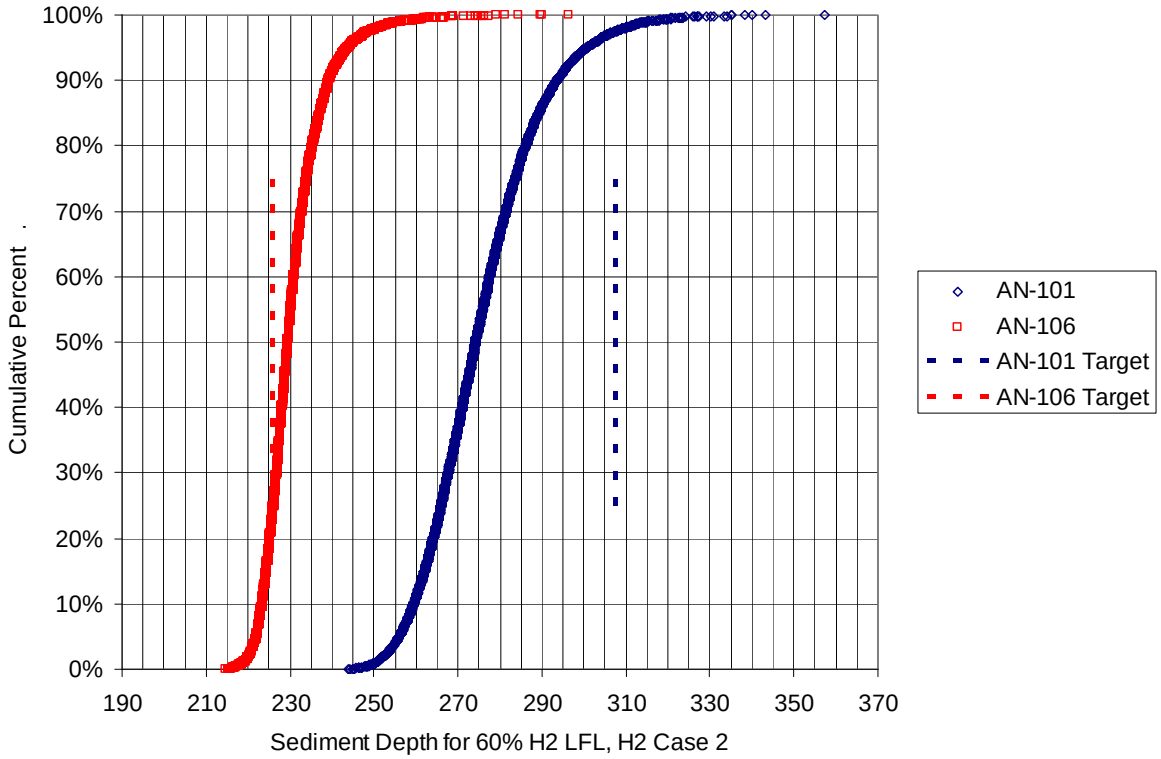


**Figure 4.2**. H2 Case 2

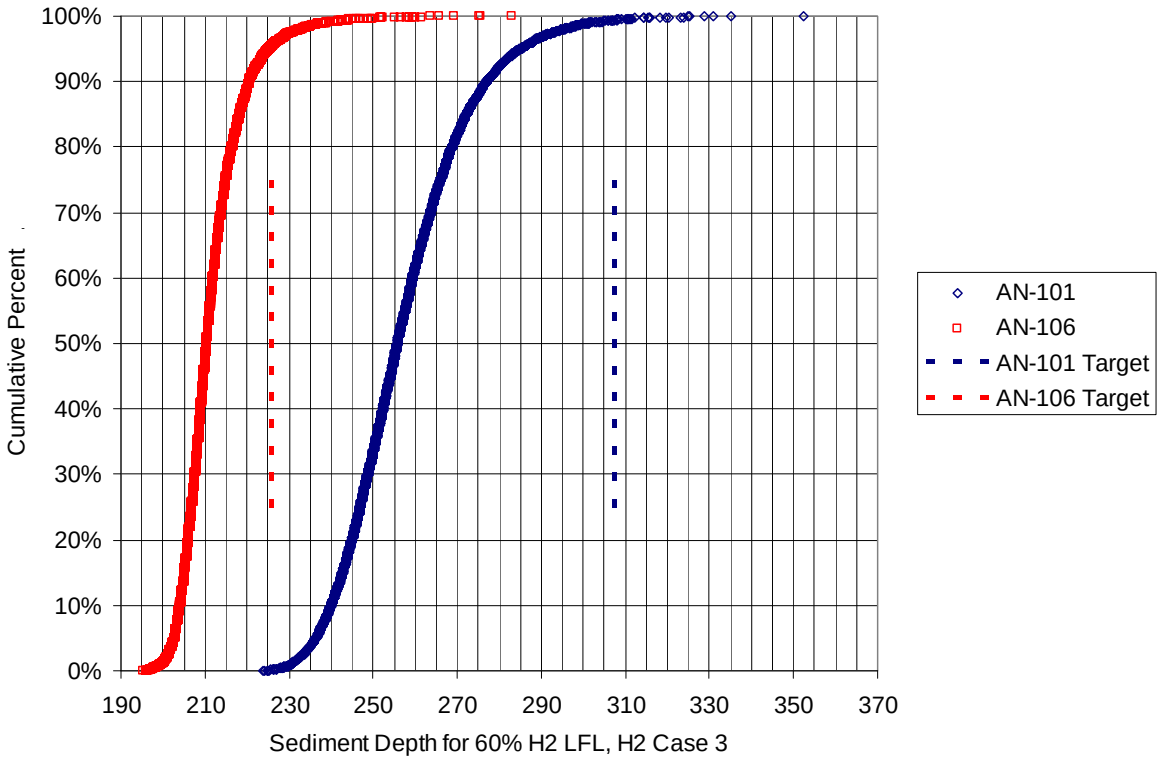


**Figure 4.3**. H2 Case 3

### 4.2.2 Effect of Peak Hydrogen Concentration in Headspace Limit

Meacham and Kirch (2013) provided an initial assessment of the potential for flammable GREs in DSTs that contain deep sludge layers. Their conservative calculations provided for sludge accumulations in Tanks AN-101 and AN-106 used a headspace flammability limit of only 60% of the LFL (neglecting the contribution of other flammable gases).

The limiting sediment depth for 100% LFL is evaluated for comparison to the conservative 60% limit for $[H_2]_{peak}$ (Equation (2.3)). Two LFL cases (60% of the LFL and 100% of the LFL) for sediment depths that limit the hydrogen concentration in the headspace are computed through the Monte Carlo simulation for the parameter values. The limiting sediment depths for LFL Case 1 are already shown in Figure 4.1 and for LFL Case 2 in Figure 4.4. There is significant difference in the results. For the 60% limit (Figure 4.1), less than 5% of the predicted sediment depth results for Tank AN-101 are equal to or greater than the projected target and approximately 35% for Tank AN-106. At the 100% limit, approximately 50% of the predicted sediment depth results for Tank AN-101 are equal to or greater than the projected target, and all results for Tank AN-106 exceed the target.

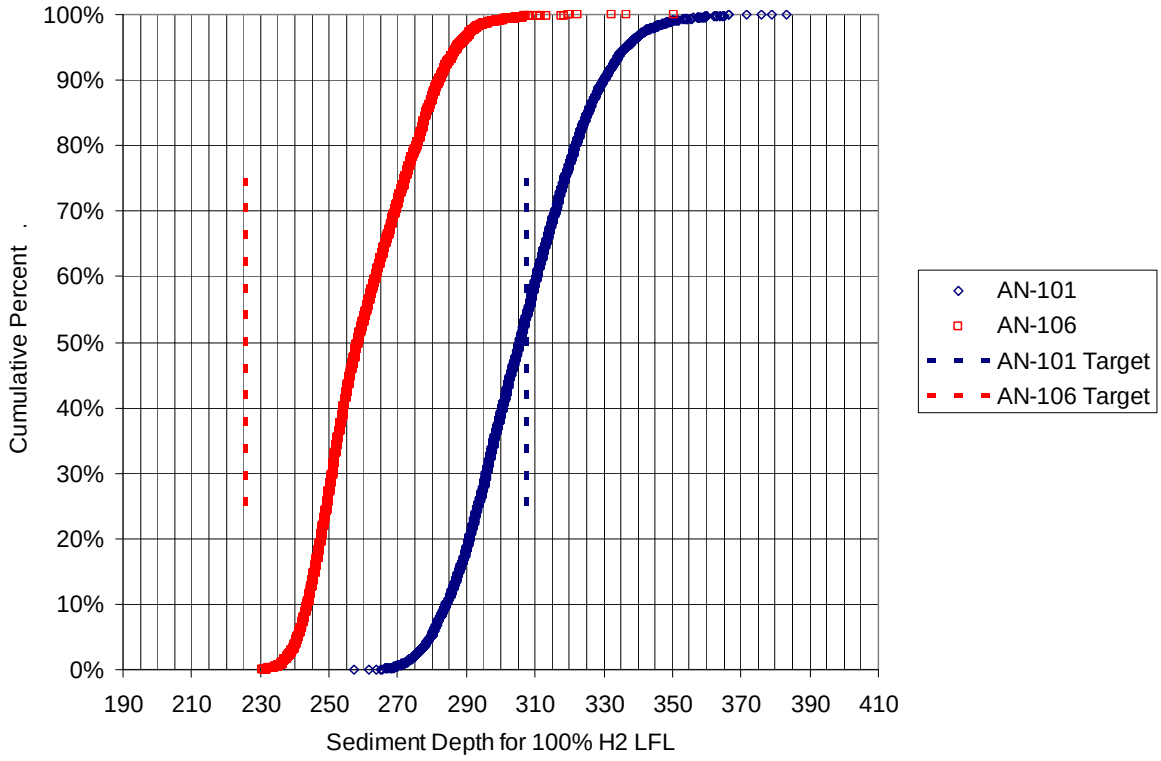


**Figure 4.4**. LFL Case 2

## 4.3 Discussion

Stewart et al. (2005) provided recommendations for applying the flammability model to address "factor of safety" or "safety limits." They noted that the limiting buoyancy ratio for specific flammability conditions defined by the tank headspace, retained gas hydrogen fraction, and limiting hydrogen concentration via Equation (2.4) can be used exactly like the current limit of BR <1 as described by Yarbrough (2013). However, for planning operations, a specialty assessment recommended a "factor of safety" of 2 be applied to ensure that later adjustments to property values or new measurements will not push the buoyancy ratio above the limit (Kirch and Meacham 2004). Stewart et al. (2005) also noted that a safety margin may be achieved by using something like the 95$^{th}$ percentile value of the buoyancy ratio calculated in a Monte Carlo simulation to compare against a limit. They concluded that the most important requirement is that the flammability model results not be used in any safety-related calculation without a full understanding of the model basis, data set, and limits of applicability which are addressed in detail in this report.

Currently, the DSA controls that prevent potential GRE flammable gas hazards from large spontaneous BDGREs apply three criteria (see Section 1) through a Monte Carlo methodology (Yarbrough 2013). For the buoyancy ratio model control, which is based on an understanding of the BDGRE tank behavior, it is required that the buoyancy ratio must be less than unity for >95% of the Monte Carlo simulation results. The value of unity is the discriminating value for BDGRE behavior: BR<1, BDGREs do not occur; BR≥1, BDGREs occur. The approach is the same for the energy ratio

limit (which is again based, in part, on the BDGRE tank behavior). The third DSA control for preventing BDGRE flammable gas hazards is based on the retained gas volume. As stated in Yarbrough (2013):

> "This criterion determines whether the tank contains sufficient retained gas such that the well-mixed headspace flammable gas concentration would reach 100% of the LFL if the entire tank's retained gas were released. If there is not sufficient retained gas to reach 100% of the LFL, then flammable conditions cannot be reached and the tank is classified as a waste group C tank independent of the gas release method."

It follows that it would be consistent with the current DSA methodology to control the potential headspace concentrations from spontaneous GREs based on the flammability model to 100% of the LFL (i.e., LFL Case 2, Figure 4.4) not to the 60% of the LFL limit of Meacham and Kirch (2013).

Given that the flammability model is conservative (it is derived from the upper bound of the 95% confidence interval of the best quadratic model fit to the 95$^{th}$ percentile peak hydrogen concentration estimates, Section 2.1), this approach of using LFL Case 2 is arguably more conservative than the current DSA controls with respect to the models' bases of BDGRE tank behavior and parameters. Essentially the same uncertainties relative to behavior and waste parameters exist in the DSA models as the flammability model.

The discrimination for the buoyancy ratio, however, is the limit of whether an event will occur or not, not whether the occurrence of an event will be "safe." The energy ratio is more similar to the flammability model in that the limit prescribes when the occurrence of a buoyant displacement will not cause the release of gas so, in effect, it limits the GRE to 0% LFL. The Yarbrough (2013) methodology, as noted, employs all three criteria concurrently. Thus, for a tank to have a flammable gas hazard, it must have enough retained gas such that the headspace flammable gas concentration would reach 100% of the LFL if the entire tank's retained gas were released, it must fail the energy ratio criteria, and it must fail the buoyancy ratio criteria.

Uytioco (2011) provides supernatant liquid depth limits for Tanks AN-101 and AN-106 at projected retrieval conditions via the waste grouping flammability controls specified in Yarbrough (2013). The conditions used for the current analysis of the flammability model are conservative with respect to the Uytioco (2011) analysis (Section 3.3). The application of the flammability model at 100% LFL to a tank configuration that meets the DSA controls which prevent potential GRE flammable gas hazards from large spontaneous BDGREs is therefore meaningful, and the results of LFL Case 2 are further discussed.

From Figure 4.4 (LFL Case 2), approximately 50% of the predicted sediment depth results for Tank AN-101 are equal to or greater than the projected target, and all results for Tank AN-106 exceed the target. These results indicate that the largest spontaneous GREs at the projected target conditions in Tank AN-106 will not exceed 100% of the LFL for any results of the simulated distribution. For Tank AN-101, the median of the predicted sediment depths is at the sediment depth target. That is, the most probable result is that the largest spontaneous GREs at the target waste depth will not exceed 100% of the LFL, but there is a 50% chance that 100% of the LFL could be exceeded were the sediment depth raised to the target depth. A reasonable limit can be established for the Tank AN-101 sediment depth following the 95$^{th}$ percentile safety margin suggestion of Stewart et al. (2005). To have 95% of the predicted sediment depths result in less than 100% of the LFL, the 5$^{th}$ percentile of the Tank AN-101 results of Figure 4.4 is specified (approximately 280 in.).

To summarize, from the Stewart et al. (2005) flammability model with the limiting headspace hydrogen concentration at 100% of the LFL, the calculated allowable sediment depth in Tank AN-101 is 280 in. and 226 in. for Tank AN-106. As described, the bases for these predictions are the gas release behavior of the BDGRE tanks. Therefore, these new model results should only be used in combination with other planned studies of DSGRE behavior to address the range of potential releases. An aspect of these planned studies is to investigate the gas releases from DSGREs. If the gas releases from DSGREs based on the results from the planned studies are smaller than would be expected for BDGREs, the flammability model bounds the potential gas releases from the deep sludge in Tanks AN-101 and AN-106.

The conservative calculations of Meacham and Kirch (2013) evaluated the layer depth allowed if:

1. the layer is at the bottom of the sediment
2. the DSGRE encompasses the tank area
3. the layer is neutrally buoyant with respect to the supernatant liquid
4. the fraction of the gas released from this layer is equal to the largest BDGRE release fraction
5. the hydrogen fraction in the retained gas is 0.47
6. the release will not exceed 60% of the LFL.

As these assumptions lead to more restrictive sediment depths than the flammability model results (Tank AN-101, 192.5 in. compared to 220 in., $0^{th}$ percentile, Figure 4.1; Tank AN-106, 195.4 in. compared to 195 in., $0^{th}$ percentile, Figure 4.1), it can be concluded that BDGREs (i.e., the flammability model) do not bound DSGREs (i.e., Meacham and Kirch 2013) at the equivalence of assumption 6. The assumptions of Meacham and Kirch (2013) are compared to BDGRE behavior to investigate this potential conclusion.

For assumption 1, the measured linear gas fraction profiles with sediment depth in the BDGRE tanks (Meyer et al. 1997; Hedengren et al. 2000) show that the lower sediment depths can have larger gas concentrations, so the Meacham and Kirch (2013) DSGRE condition is in agreement with the BDGRE tank data (the flammability model basis). With respect to assumption 2, Wells et al. (2002) determined that the historically observed BDGREs were in fact not single events but the combination of multiple buoyant displacements. The phenomenon triggering the multiple displacement events was the decrease in neutral buoyancy as the previous events added suspended solids to the supernatant liquid. Wells et al. (2002) assumed that the buoyant sediment extended the depth of the sediment (as supported by the gas fraction profiles), and thus, based on the Rayleigh-Taylor stability analysis conducted by Meyer et al. (1997), concluded that the most probable diameter of a buoyant displacement was equal to the sediment depth. Because the BDGREs were the combination of multiple displacement events, the largest of the individual events must have been smaller radially than the tank diameter (Wells et al. (2002) used half the tank diameter as the maximum diameter). Therefore, the assumption that a DSGRE will involve the entire tank area may be conservative. Note that the largest BDGREs in the flammability model likely did encompass most of the tank area via multiple displacements, but there was the additional driver of altered neutral buoyancy to "trigger" subsequent events. The DSGRE assumption 1 is in agreement with the flammability model basis, but assumption 2 may be overly conservative. Comparison of the retained gas volume relative to assumption 2 is made below regarding assumption 3.

Meacham and Kirch (2013) evaluated the DSGREs at neutral buoyancy gas fractions of 0.295 for Tank AN-101, and 0.308 for Tank AN-106 (assumption 3). Comparison to Figure 3.4 shows that nearly all the flammability model simulations for Tank AN-101 had higher neutral buoyant gas fractions (as part of the buoyancy ratio), while all the simulations for Tank AN-106 were lower, with the maximum neutral buoyancy approximately equivalent. The flammability model neutral buoyancy gas fractions, as represented through the measured BDGRE tank data with parabolic or linearly increasing gas fraction with depth (Meyer et al. 1997; Hedengren et al. 2000), require that the linear gas fractions actually have greater than neutral buoyancy at the bottom of the sediment because the average gas fraction must be neutrally buoyant (see Wells et al. 2002). In addition, the entire sediment depth is participating in the displacement event (Wells et al. 2002; Stewart et al. 2005), so the quantity of gas available to be released is significant.

The gas fraction at the bottom of the sediment with an average gas fraction of the minimum neutral buoyancy for Tank AN-106 of approximately 0.23 (Figure 3.4) is 0.46 (linear gas fraction profile). For a 5.7-meter (226 in.) sediment, this equates to approximately 542 $m^3$ of retained gas in the sediment, or 136 $m^3$ in a displacement with a diameter of half the tank diameter (again at in situ conditions). For the Meacham and Kirch (2013) DSGRE in Tank AN-106, the buoyant sediment depth limit was 0.6 meters (23.4 in.). With a 0.308 gas fraction, the retained gas volume is approximately 75 $m^3$. Equating the gas volumes via pressure corrections to the top of the sediment (the same supernatant liquid depths were used in both analyses), the BDGRE volume is 190 $m^3$, and the DSGRE volume is 128 $m^3$. It is therefore concluded that the retained gas volumes for the sediment undergoing a BDGRE (as represented by the flammability model; note that the minimum neutral buoyancy condition is used for comparison) are likely larger than that assumed for the DSGRE. The flammability model basis thus bounds the DSGRE assumption 3 and negates the effect of assumption 2.

For assumption 4, Meacham and Kirch (2013) assigned the largest release fraction of the BDGRE tanks. This event is included in the flammability model development, and, as shown in Figure 2.1, the expression at 100% of the LFL (40,000 ppm "Peak $[H_2]$") represents the lower (BR-1)$[H_2]_{gas}/V_{HS}$ values for the largest releases ("95%ile BDGREs") well. Therefore, the flammability model basis includes the data used for DSGRE assumption 4.

The effect of assumption 5 is evaluated for both the flammability model (Section 4.2.1) and the DSGRE releases (Meacham and Kirch 2013) and has a significant impact on the results. The Meacham and Kirch (2013) value is comparable to the 50$^{th}$ percentile value used in the flammability model, Figure 3.7. 50% of the simulated sediment depth predictions from the flammability model are at lower hydrogen concentrations in the retained gas and 50% are higher (up to two times higher). As a result, the span of the flammability model simulation results is more conservative.

These DSGRE assumption comparisons to the flammability model bases and predictions demonstrate the possible conclusion from the Meacham and Kirch (2013) results that BDGREs do not bound DSGREs is incorrect. Rather, the approaches are based on similar assumptions, conservative results are similar, and the difference in the results is attributable to the differences in the parameter values as well as the combination of conservatism (DSGRE approach) vs. correlation to tank data (flammability model).

# 5.0 Conclusions

Meacham and Kirch (2013) proposed a new mechanism for a large spontaneous GRE in deep sludge Hanford tank waste sediments. The source of this potential new GRE hazard (DSGREs) is the retrieval of sludge waste into a single DST that results in a sediment depth greater than operating experience has demonstrated is safe. The Tank Operations Contractor program of moving solid wastes from SSTs to DSTs and preparing for WFD is being negatively impacted by this sediment depth limit.

One approach to evaluate the hazard is to estimate the effect of this new waste configuration relative to the spontaneous GRE events that have been observed in the Hanford tank farms, the largest of which are attributed to BDGREs. An empirical model based on tank farm spontaneous GRE data and waste properties to predict the flammable gas (specifically hydrogen) concentration in a tank's headspace is available (Stewart et al. 2005). This flammability model has been applied to the anticipated conditions resulting from C Tank Farm sludge retrieval into Tanks AN-101 and AN-106. Based on historical Hanford waste spontaneous gas release volumes, the allowed depth of sludge in Tanks AN-101 and AN-106 has been determined that will limit headspace hydrogen concentrations to a given fraction of the LFL.

For the projected retrievals of C Tank Farm waste into AN Tank Farm, there are no actual waste data, and the waste characteristics have been estimated. To account for the uncertainty in the data, the values used in this study have been assigned distributions that reflect the uncertainty in the estimation of the various tank waste properties and a Monte Carlo methodology was employed to calculate simulated distributions of sediment depth values (as it relates to the flammability model).

The Stewart et al. (2005) model is based on the large BDGREs that occur in a limited number of the Hanford waste tanks. The projected waste characteristic for retrievals of C Tank Farm waste into AN Tank Farm was evaluated with respect to the flammability model bases, and it was concluded that no adjustments need to be made to the flammability model.

Through comparison to the DSA, it was deemed that the application of the flammability model at 100% LFL is applicable for a tank configuration that meets the DSA controls that prevent potential GRE flammable gas hazards from large spontaneous BDGREs. From the Monte Carlo simulations performed with the Stewart et al. (2005) flammability model, the allowable sediment depth in Tank AN-101 was calculated to be 280 in. and 226 in. in Tank AN-106. The bases for these predictions are the gas release behavior of the BDGRE tanks, but comparison to the conservative analysis of DSGREs (Meacham and Kirch 2013) does not suggest that DSGREs will be larger than BDGREs. However, the model results in this report should only be used in combination with other planned studies of DSGRE behavior to address the range of potential releases. If the gas releases from DSGREs based on the results from the other planned studies are smaller than would be expected for BDGREs, the flammability model bounds the potential gas releases from the deep sludge in Tanks AN-101 and AN-106.

# 6.0 References

10 CFR 830, Subpart A. 2010. "Nuclear Safety Management." Subpart A, "Quality Assurance Requirements." *Code of Federal Regulations*, U.S. Department of Energy.

Antoniak ZI. 1993. *Historical Trends in Tank 241-SY-101 Waste Temperatures and Levels.* PNL-8880, Pacific Northwest Laboratory, Richland, Washington.

Barton WB, JM Grigsby, JE Meacham, TL Sams, and RB Calmus. 2013. *Report of the Deep Sludge Gas Release Event Technical Meeting, Denver, Colorado March 26 - 28, 2013*. RPP-RPT-54941 Rev. 0, Washington River Protection Solutions, LLC, Richland, Washington.

DOE Order 414.1D. 2011. "Quality Assurance." U.S. Department of Energy, Washington, D.C.

Gauglitz PA, BE Wells, JA Fort, and PA Meyer. 2009. *An Approach to Understanding Cohesive Slurry Settling, Mobilization, and Hydrogen Gas Retention in Pulsed Jet Mixed Vessels*. PNNL-17707; WTP-RPT-177 Rev. 0, Pacific Northwest National Laboratory, Richland, Washington.

Gauglitz PA and JT Aikin. 1997. *Waste Behavior During Horizontal Extrusion: Effect of Waste Strength for Bentonite and Kaolin/Ludox Simulants and Strength Estimates for Wastes from Hanford Tanks 241-SY-103, AW-101, AN-103, and S-102*. PNNL-11706, Pacific Northwest National Laboratory, Richland, Washington.

Harrington SJ. 2013. *Double-Shell Tanks 241-AN-101 and 241-AN-106 Bulk Density Layering from C-Farm Retrievals Through July 11, 2013*. RPP-RPT-56013 Rev. 0, Washington River Protection Solutions, LLC, Richland, Washington.

Hedengren DC, KM Hodgson, WB Barton, CW Stewart, JM Cuta, and BE Wells. 2000. *Data Observations on Double-Shell Flammable Gas Watch List tank Behavior*. RPP-6655, CH2M HILL Hanford Group, Inc., Richland, Washington.

Hester JR. 2002. *Radiolytic Bubble Gas Hydrogen Compositions.* WSRC-TR-2001-00193, Westinghouse Savannah River Company, Savannah River Site, Aiken, South Carolina.

Hu TA. 2006. *Methodology and Calculations for the Assignment of Waste Groups for the Large Underground Waste Storage Tanks at the Hanford Site*, RPP-10006 Rev. 6, Washington River Protection Solutions LLC, Richland, Washington.

Kirch NW and JE Meacham. 2004. *Flammable Gas Waste Group Assignment FY2004-ENG-S-0133.* RPP-21336, CH2M HILL Hanford Group, Inc., Richland, Washington.

Kripps LJ. 2011. *Tank Farms Documented Safety Analysis*. RPP-13033. As amended. Washington River Protection Solutions LLC, Richland, Washington.

Mahoney LA. 2000. *Ammonia Results Review for Retained Gas Sampling*. PNNL-13317, Pacific Northwest National Laboratory, Richland, Washington.

Meacham JE. 2010. *Gas Retention and Release from Hanford Site High Shear Strength Waste*. RPP-RPT-26836 Rev. 0, Washington River Protection Solutions, LLC, Richland, Washington.

Meacham JE and NW Kirch. 2013. *Initial Assessment for Potential Gas Release Events in Hanford Site Deep Sludge Double-Shell Tank Waste*. RPP-RPT-54305 Rev. 0, Washington River Protection Solutions LLC, Richland, Washington.

Meacham JE, SJ Harrington, JS Rodriquez, VC Nguyen, JG Reynolds, BE Wells, GF Piepel, SK Cooley, CW Enderlin, DR Rector, J Chun, A Heredia-Langner, and RF Gimpel. 2012. *One System Evaluation of Waste Transferred to the Waste Treatment Plant*. RPP-RPT-51652 Rev. 0; PNNL-21410, Washington River Protection Solutions LLC, Richland, Washington.

Meyer PA and CW Stewart. 2001. *Preventing Buoyant Displacement Gas Release Events in Hanford Double-Shell Waste Tanks*. PNNL-13337, Pacific Northwest National Laboratory, Richland, Washington.

Meyer PA, LR Pederson, ME Brewster, CW Stewart, SA Bryan, G Terrones, and G Chen. 1997. *Gas Retention and Release Behavior in Hanford Double-Shell Waste Tanks*. PNNL-11536 Rev. 1, Pacific Northwest National Laboratory, Richland, Washington.

Occurrence Report EM-RP--WRPS-TANKFARM-2012-0014. 2012. "Potential Exists for a Large Spontaneous Gas Release Event in Deep Settled Waste Sludge." Washington River Protection Solutions, LLC, Richland, Washington.

Rassat SD, LA Mahoney, BE Wells, DP Mendoza, and DD Caldwell. 2003. *Assessment of Physical Properties of Transuranic Waste in Hanford Single-Shell Tanks*. PNNL-14221, Pacific Northwest National Laboratory, Richland, Washington.

Stevens KK. 1979. *Statics and Strength of Materials*. ISBN 0-13-844688-1, Prentice-Hall, Inc., Englewood Cliffs, New Jersey.

Stewart CW, SA Hartley, PA Meyer, and BE Wells. 2005. *Predicting Peak Hydrogen Concentrations from Spontaneous Gas Releases in Hanford Waste Tanks*. PNNL-15238, Pacific Northwest National Laboratory, Richland, Washington.

Stewart CW, PA Meyer, ME Brewster, KP Recknagle, PA Gauglitz, HC Reid, and LA Mahoney. 1996. *Gas Retention and Release Behavior in Hanford Single-Shell Waste Tanks*. PNNL-11391, Pacific Northwest National Laboratory, Richland Washington.

Stock LM. 2001. *The Chemistry of Flammable Gas Generation*. RPP-6664 Rev. 1, CH2M HILL Hanford Group, Inc., Richland, Washington.

Uytioco EM. 2011. *BDGRE and Supernatant Limit Assessment for Enhanced Use of AN Farm for C Farm Single Shell Tank Retrieval*. RPP-RPT-44254 Rev. 1, Washington River Protection Solutions, LLC, Richland, Washington.

van Kessel T and WGM van Kesteren. 2002. "Gas Production and Transport in Artificial Sludge Depots." *Waste Management* 22(1):19–28.

Wells BE, DE Kurath, LA Mahoney, Y Onishi, JL Huckaby, SK Cooley, CA Burns, EC Buck, JM Tingey, RC Daniel, and KK Anderson. 2011. *Hanford Waste Physical and Rheological Properties: Data and Gaps*. PNNL-20646, Pacific Northwest National Laboratory, Richland Washington.

Wells BE, RL Russell, LA Mahoney, GN Brown, DE Rinehart, WC Buchmiller, EC Golovich, and JV Crum. 2010a. *Hanford Sludge Simulant Selection for Soil Mechanics Property Measurement*. PNNL-19250, Pacific Northwest National Laboratory, Richland, Washington.

Wells BE, JJ Jenks, G Boeringa, NN Bauman, and AD Guzman. 2010b. *Lateral Earth Pressure at Rest and Shear Modulus Measurements on Hanford Sludge Simulants*. PNNL-19829, Pacific Northwest National Laboratory, Richland, Washington.

Wells BE, JM Cuta, SA Hartley, LA Mahoney, PA Meyer, and CW Stewart. 2002. *Analysis of Induced Gas Releases During Retrieval of Hanford Double-Shell Tank Waste*. PNNL-13782, Pacific Northwest National Laboratory, Richland, Washington.

Winterwerp JC and WGM van Kesteren. 2004. *Introduction to the Physics of Cohesive Sediment in the Marine Environment*. Elsevier B. V., Amsterdam, The Netherlands.

WRPS-PER-2012-2007. 2012. *Large Spontaneous Gas Release Event (GRE) in Deep Settled Sludges*. Washington River Protection Solutions, Richland, Washington.

Yarbrough RJ. 2013. *Methodology and Calculations for the Assignment of Waste Groups for the Large Underground Waste Storage Tanks at the Hanford Site*. RPP-10006 Rev. 11, Washington River Protection Solutions LLC, Richland, Washington.

# Distribution

**No. of Copies**

2 **DOE Office of River Protection**

| | |
|---|---|
| JS Shuen | H6-60 |
| BJ Stickney | H6-60 |

7 **Washington River Protection Solutions**

| | |
|---|---|
| WE Bryan | H3-20 |
| RB Calmus | H8-04 |
| JM Grigsby | S7-90 |
| SJ Harrington | R2-58 |
| NW Kirch | R2-58 |
| JE Meacham | R2-58 |
| TL Sams | R2-52 |

**No. of Copies**

12 **Pacific Northwest National Laboratory**

| | |
|---|---|
| SK Cooley | K7-20 |
| RC Daniel | P7-22 |
| JA Fort | K7-15 |
| PA Gauglitz (4) | K7-15 |
| MR Powell | K6-24 |
| SD Rassat | K6-28 |
| DR Rector | K7-15 |
| PP Schonewill | P7-25 |
| BE Wells | K7-15 |

Pacific Northwest
NATIONAL LABORATORY

U.S. DEPARTMENT OF
ENERGY

*Proudly Operated by* Battelle *Since 1965*

902 Battelle Boulevard
P.O. Box 999
Richland, WA 99352
1-888-375-PNNL (7665)
www.pnl.gov